ISSN 2444-4987

Journal of Research and Development

Volume 7, Issue 19 — January — June - 2021

ECORFAN®

Journal of Research and Development, Volume 7, Issue 19, January – June 2021, is a journal edited semestral by ECORFAN-Spain. 38 Matacerquillas, CP-28411. Moralzarzal – Madrid-España. WEB: www.ecorfan.org/spain, revista@ecorfan.org. Editor in Chief: VARGAS-DELGADO, Oscar. PhD. ISSN: 2444-4987. Responsible for the last update of this number of the ECORFAN Computing Unit. ESCAMILLA–BOUCHÁN, Imelda. PhD, LUNA-SOTO, Vladimir. PhD, updated to June 30, 2021.

Journal of Research and Development

Definition of Journal

Scientific Objectives

Support the international scientific community in its written production Science, Technology and Innovation in the Field of Humanities and Behavioral Sciences, in Subdisciplines of industrial development, project model, computer application, research production, systems development, research networks, application design, programming and development proposals.

ECORFAN-Mexico SC is a Scientific and Technological Company in contribution to the Human Resource training focused on the continuity in the critical analysis of International Research and is attached to CONACYT-RENIECYT number 1702902, its commitment is to disseminate research and contributions of the International Scientific Community, academic institutions, agencies and entities of the public and private sectors and contribute to the linking of researchers who carry out scientific activities, technological developments and training of specialized human resources with governments, companies and social organizations.

Encourage the interlocution of the International Scientific Community with other Study Centers in Mexico and abroad and promote a wide incorporation of academics, specialists and researchers to the publication in Science Structures of Autonomous Universities - State Public Universities - Federal IES - Polytechnic Universities - Technological Universities - Federal Technological Institutes - Normal Schools - Decentralized Technological Institutes - Intercultural Universities - S & T Councils - CONACYT Research Centers.

Scope, Coverage and Audience

Journal of Research and Development is a Journal edited by ECORFAN-Mexico S.C in its Holding with repository in Spain, is a scientific publication arbitrated and indexed with semester periods. It supports a wide range of contents that are evaluated by academic peers by the Double-Blind method, around subjects related to the theory and practice of industrial development, project model, computer application, research production, systems development, research networks, application design, programming and development proposals with diverse approaches and perspectives , That contribute to the diffusion of the development of Science Technology and Innovation that allow the arguments related to the decision making and influence in the formulation of international policies in the Field of Humanities and Behavioral Sciences. The editorial horizon of ECORFAN-Mexico® extends beyond the academy and integrates other segments of research and analysis outside the scope, as long as they meet the requirements of rigorous argumentative and scientific, as well as addressing issues of general and current interest of the International Scientific Society.

Arbitration Committee

Assignment of Rights

The sending of an Article to Journal of Research and Development emanates the commitment of the author not to submit it simultaneously to the consideration of other series publications for it must complement the Originality Format for its Article.

The authors sign the Authorization Format for their Article to be disseminated by means that ECORFAN-Mexico, S.C. In its Holding Spain considers pertinent for disclosure and diffusion of its Article its Rights of Work.

Declaration of Authorship

Indicate the Name of Author and Coauthors at most in the participation of the Article and indicate in extensive the Institutional Affiliation indicating the Department.

Identify the Name of Author and Coauthors at most with the CVU Scholarship Number-PNPC or SNI-CONACYT- Indicating the Researcher Level and their Google Scholar Profile to verify their Citation Level and H index.

Identify the Name of Author and Coauthors at most in the Science and Technology Profiles widely accepted by the International Scientific Community ORC ID - Researcher ID Thomson - arXiv Author ID - PubMed Author ID - Open ID respectively.

Indicate the contact for correspondence to the Author (Mail and Telephone) and indicate the Researcher who contributes as the first Author of the Article.

Plagiarism Detection

All Articles will be tested by plagiarism software PLAGSCAN if a plagiarism level is detected Positive will not be sent to arbitration and will be rescinded of the reception of the Article notifying the Authors responsible, claiming that academic plagiarism is criminalized in the Penal Code.

Arbitration Process

All Articles will be evaluated by academic peers by the Double Blind method, the Arbitration Approval is a requirement for the Editorial Board to make a final decision that will be final in all cases. MARVID® is a derivative brand of ECORFAN® specialized in providing the expert evaluators all of them with Doctorate degree and distinction of International Researchers in the respective Councils of Science and Technology the counterpart of CONACYT for the chapters of America-Europe-Asia- Africa and Oceania. The identification of the authorship should only appear on a first removable page, in order to ensure that the Arbitration process is anonymous and covers the following stages: Identification of the Journal with its author occupation rate - Identification of Authors and Coauthors - Detection of plagiarism PLAGSCAN - Review of Formats of Authorization and Originality-Allocation to the Editorial Board-Allocation of the pair of Expert Arbitrators-Notification of Arbitration -Declaration of observations to the Author-Verification of Article Modified for Editing-Publication.

Instructions for Scientific, Technological and Innovation Publication

Knowledge Area

The works must be unpublished and refer to topics of industrial development, project model, computer application, research production, systems development, research networks, application design, programming and development proposals and other topics related to Humanities and Behavioral Sciences.

Presentation of the Content

In the first chapter we present, *Design of edges in contour and half moons from edaphoclimatic parameters, for the endorrheic basin of lagunas de tajzara - ramsar site 1030*, by SCHMIDT-GOMEZ, Armando, OLIVARES-RAMÍREZ, Juan Manuel, FERRIOL-SÁNCHEZ, Fermín and MARROQUÍN-DE JESÚS, Ángel, with adscription in the Universidad Internacional Iberoamericana and the Universidad Tecnológica de San Juan del Río, as next article we present, *Active disturbance rejection control of a permanent magnet synchronous generator for wind turbine applications*, by AGUILAR-ORDUÑA, Mario Andrés & SIRA-RAMÍREZ, Hebertt José, with adscription in the Centro de Investigación y de Estudios Avanzados del Instituto Politécnico Nacional (CINVESTAV), as next article we present, *Implementation of improvement actions in a company that produces frames and moldings*, by FORNÉS-RIVERA, René Daniel, CONANT-PABLOS - Marco Antonio, CANO-CARRASCO Adolfo and LÓPEZ-ROJO, Gildardo Guadalupe, with adscription in the Instituto Tecnológico de Sonora, as next article we present, *Design and simulation of Dynamic Voltage Restorer (DVR) supported by solar panels* by ANTONIO-LARA, Omar, GARCÍA-VITE, Pedro Martín, CASTILLO-GUTIÉRREZ, Rafael and CISNEROS-VILLEGAS, Hermenegildo, with adscription in the Instituto Tecnológico de Ciudad Madero.

Content

Article **Journal of Research and Development**
June, 2021 Vol.7 No.19 1-8

Design of edges in contour and half moons from edaphoclimatic parameters, for the endorrheic basin of lagunas de tajzara - ramsar site 1030

Diseño de bordes en contorno y medias lunas a partir de parámetros edafoclimáticos, para la cuenca endorreica de las lagunas de tajzara - sitio ramsar 1030

SCHMIDT-GOMEZ, Armando[1], OLIVARES-RAMÍREZ, Juan Manuel[2], FERRIOL-SÁNCHEZ, Fermín[1] and MARROQUÍN-DE JESÚS, Ángel[2]

Universidad Internacional Iberoamericana, Facultad de Ingeniería, Campeche 24560, México
Universidad Tecnológica de San Juan del Río, Querétaro 76800, México

ID 1st Author: *Armando, Schmidt-Gomez* / **ORC ID**: 0000-0002-9433-126X

ID 1st Co-author: *Juan Manuel, Olivares-Ramírez* / **ORC ID**: 0000-0003-2427-6936

ID 2nd Co-author: *Fermín, Ferriol-Sánchez* / **ORC ID**: 0000-0003-4138-8999

ID 3rd Co-author: *Ángel, Marroquín-De Jesús* / **ORC ID**: 0000-0001-7425-0625

DOI: 10.35429/JRD.2021.19.7.1.8 Received March 02, 2021; Accepted June 29, 2021

Abstract

The collection of water is proposed from the design of contour borders and half moons, green infrastructure measures, to reduce surface runoff and increase the availability of water for vegetation. The contour and crescent ridges have land ridges with a trapezoidal section, which follow the contour lines, to compartmentalize the slope into smaller hydrological units, the ends of which are located on contour lines. With the data of maximum rainfall every 24 hours and parameters of Gumbel's Law modified, the equations of maximum daily rainfall height (hdT), rainfall height for a duration ´´t´´ (htT), and the Intensity Duration Frequency curve (ItT), for a duration of t <2h. Then considering the values of basic infiltration, vegetation cover, soil type and hydrological condition, the curve numbers were determined for different soil moisture conditions, later the separation length (L) between the Half Moons, and the borders was calculated. in contour, which were designed by means of 10 configurations between diameter and height, for the two infrastructures, being in Copacabana Valle, the greatest separation distance.

Infiltration, Crescent moons, Borders in contour

Resumen

Se plantea la captación del agua a partir del diseño de bordos en contorno y media lunas, medidas de infraestructura verde, para disminuir el escurrimiento superficial e incrementar la disponibilidad de agua para la vegetación. Los bordos en contorno y media lunas presentan caballones de tierra con sección trapezoidal, que siguen las curvas de nivel, para compartimentar la ladera en unidades hidrológicas más pequeñas, cuyos extremos se sitúan sobre curvas de nivel. Con los datos de precipitaciones máximas cada 24 horas y parámetros de la Ley de Gumbel modificada, se obtuvieron las ecuaciones de altura de lluvia máxima diaria, (h_{dT}), altura de lluvia para una duración ´´t´´(h_{tT}), y la curva Intensidad Duración Frecuencia (I_{tT}), para una duración de t<2h. Luego considerando los valores de infiltración básica, cubierta vegetal, tipo de suelo y condición hidrológica, se determinaron los números de curva para diferentes condiciones de humedad del suelo, posteriormente se calculó la longitud de separación (L) entre las Media Lunas, y los bordos en contorno, mismas que se diseñaron mediante 10 configuraciones entre el diámetro y la altura, para las dos infraestructuras, encontrándose en Copacabana Valle, la mayor distancia de separación.

Infiltración, Media lunas, Bordos en contorno

Citation: SCHMIDT-GOMEZ, Armando, OLIVARES-RAMÍREZ, Juan Manuel, FERRIOL-SÁNCHEZ, Fermín and MARROQUÍN-DE JESÚS, Ángel. Design of edges in contour and half moons from edaphoclimatic parameters, for the endorrheic basin of lagunas de tajzara - ramsar site 1030. Journal of Research and Development. 2021. 7-19: 1-8

* Correspondence to Author (e-mail: jmolivar01@yahoo.com)
† Researcher contributing as first author.

1. Introduction

The high animal load supported by water recharge areas in the endorheic Tajzara basin has produced considerable degradation of the soil and vegetation, with a worrying decrease in water recharge flows. [10] Causing the ecological imbalance in the different ecosystems, which are manifested in: a) the gradual disappearance of desirable plant species, b) the decrease in plant cover, c) slow recovery of flora. As an ecosystem response to the aforementioned disturbance, invasive plant species of low nutritional value appear (successional regression), the consequence of which is the loss of forage capacity and the quality of native pastures, which is manifested in the weakness of the animals and their little resistance against diseases and low production of meat and wool [14].

[8] In the case of degraded grasslands in the basin, they mention, surface runoff can be managed to increase water availability, and promote the development of grasslands and shrubs with higher forage value, favor infiltration and increase recharge flows. subsurface and underground hydric. In addition, it is essential to know the autoecology of the species, which is associated with climatic and edaphological conditions, as well as the altitudinal distribution. [15]

On the other hand [3] they explain that this is achieved by concentrating and storing rainwater in the form of runoff in a certain space. According to [9], runoff collection systems consist of an impluvium area, which generates runoff, and a reception area, which receives runoff water. In the case of the endorheic basin of Tajzara, tholares and pastures of higher forage value will be planted in the reception area, whose water needs will be satisfied by the surface runoff captured in the impluvium area, contributing to increase the useful life of the land. that every year decreases and this is due to natural phenomena and human activity. [1]

According to [13], the water storage capacity is given mainly by the height of the board, and by the volume excavated to form the small dam, to mitigate the fact that the board has to support the entire volume of interior water. In addition, Analyze the challenges of adaptation in the framework of water management in the face of climate change [12]

2. Methodology

The Lagunas de Tajzara endorheic basin, internationally known as the Ramsar 1030 site, is located in the second municipal section of the Avilés province of the Tarija department, Bolivia, it has an area of 47,233.20 ha. At an altitude of 3,400 meters above sea level [11].

Climate exerts great influence on the environment, acting as an interaction factor between biotic and abiotic components [6]. Among the criteria, they consider texture as a parameter related to the water retention capacity and its permeability [2], in the face of the erosion process in the adopted hydrological design, for infiltration ditches, because it is a water collection system oriented to redistribute surface runoff towards water recharge, while Bordos en Contour (BC) and Media Moons (ML) are systems to retain runoff and increase water availability in the restoration of vegetation cover, based on the following calculation sequence:

- Obtaining the curves I-D-F, for rains of maximum intensity.
- Calculation of the design rain for a certain duration and return period.
- Quantification of surface runoff, according to the hydrological conditions of the soil, infiltration capacity and vegetation cover.
- Determination of the length of separation between the collection systems, considering the magnitude of the surface runoff and the dimensions of its storage area, based on the “non-exceedance” criterion.

The intensity of the design rain is determined by applying the equation of the I-D-F curve, obtained by the method of Modified Gumbel's Law according to the methodological criteria suggested by [10-7].

$$I_{t,T} = \frac{E_d}{t}\left(\frac{t}{t_d}\right)^{\beta} \cdot (1 + K \log T) \quad (1)$$

Where:
Ed: Modal value of the maximum daily rainfall height (mm).

$\bar{h}_{d,T}$: Average daily rainfall height (mm).

Sd: Standard deviation of maximum daily rainfall height (mm)

ISSN 2444-4987

t: Duration of rain (h).
td: Maximum duration of rain (h), for the region td = 3 h was determined.
β: Coefficient of the slope of the curve that is 0.2 for a t <2 h.
K: Modified Gumbel's Law distribution characteristic.
ni: Number of years with maximum daily rainfall for each season considered.
N: Total number of years with maximum daily rainfall of all the stations considered.
T: Return period in years.

According to the criteria of [8], a return period T = 10 years is assumed, which corresponds to a probability of occurrence of 90%, which is consistent with the useful life of the collection systems considered. Likewise, the intensity of rainfall is calculated for a duration t = 1 h, due to its magnitude is representative when incorporating maximum events to the hydrological design of the collection systems. The incorporation of events of less than 1 hour implies designing high cost systems that do not conform to an adequate cost / benefit ratio.

For the calculation of runoff from the impluvium, the suggested criterion [5] was applied, based on the methodology of the Curve Number of the US Soil Conservation Service.
When P> 0.05 S, then:

$$Q = \frac{(P - 0.05 \cdot S)^2}{P + 0.95 \cdot S} \quad (2)$$

With an initial abstraction S equal to:

$$S = \frac{25400}{CN_{II}} - 254 \quad (3)$$

Being:

Q: Drain runoff from the collection system (mm / h)
P: Maximum rain height for one hour duration (mm / h)
CNII: Curve number value for antecedent moisture condition II (USDA-NRCS, 2004).

Considering the type of vegetation, soil tillage (if necessary), hydrological condition, basic infiltration, and / or soil texture, the Curve Number (CNII) was determined by applying the computer program, Determination of Curve Numbers, designed by [7].

To calculate the length (LIII) of separation between water collection systems, they are deduced from the following expressions:

According to the principle established by [4], to size a water collection system, the continuity equation is considered; contribution - reception (Va = Vr), whose volumes of water are the following:

Volume of impluvium water:

$$V_i = Q \cdot A_i \quad (4)$$

Geometric volume of the collection system:

$$V_{SR} = h_{SR} \cdot A_{SR} \quad (5)$$

Volume of precipitation inside the collection system:

$$V_P = I_{t,T} \cdot t \cdot A_{SR} \quad (6)$$

Volume of infiltration in the reception area of the collection system:

$$V_{INF} = f_c \cdot t \cdot A_{SR} \quad (7)$$

Where:

Vi: Impluvium volume in m³.
Q: Surface runoff from implude in meters
Ai: Impluvium area in m².
V_{SR}: Volume of the collection system in m³.
h_{SR}: Height of the board in the storage of the collection system in m.
A_{SR}: Storage area of the collection system in m².
V_P: Volume of precipitation in the storage of the collection system in m.
$I_{t,T}$: Rain intensity in m / h, for a duration “t” in hours and a return period “T” in years.
V_{INF}: Infiltration volume in the collection system storage area in m³.
fc: Basic infiltration in m / h.

The individualized equations for each of the selected collection systems are the following:

a) Half Moons

For the impluvium area (Ai_{ML}) we have:

$$A_{iML} = D \cdot L + \frac{D^2}{2} \cdot \left(1 - \frac{\pi}{4}\right) \quad (8)$$

The volume of water generated in the impluvium area (Vi_{ML}) between Half Moons, will be:

$$V_{iML} = Q \cdot \left[D \cdot L + \frac{D^2}{2} \cdot (1 - \frac{\pi}{4}) \right] \quad (9)$$

The geometric volume in the storage area of the crescent (V_{ML}), is determined by:

$$V_{ML} = \frac{\pi}{8} \cdot D^2 \cdot h_{ML} \quad (10)$$

Where:

Q: Surface runoff generated in the implude in m.
D: Diameter of the crescent, which is equal to the width of the beam in m.
L: Horizontal length of separation between half moons in m.
h_{ML}: Height of the storage edge of the crescent in m.

Applying the equation of contribution - reception to the collection of water by the Crescent, we have:

$$V_{iML} + V_{PML} = V_{ML} + V_{INF} \quad (11)$$

In its developed expression it remains:

$$Q \cdot \left[D \cdot L + \frac{D^2}{2} \cdot (1 - \frac{\pi}{4}) \right] + (I_{t,T} \cdot t \cdot \frac{\pi}{8} \cdot D^2) = \frac{\pi}{8} \cdot D^2 \cdot h_{ML} + \frac{\pi}{8} \cdot D^2 \cdot f_c \cdot t$$

Where the separation length (L) between Half Moons can be obtained.

$$L = \frac{\pi \cdot D\left[h_{ML} + t \cdot (f_c + I_{t,T})\right]}{8 \cdot Q} - (1 - \frac{\pi}{4}) \quad (12)$$

The correction to calculate the length (Li) on a slope when θ >0 is:

$$L_i = \frac{L}{\cos\theta} \quad (13)$$

a) Borders in Contour

The impluvium area for Contour Borders (Ai_{BC}) is:

$$A_{iBC} = D \cdot L \quad (14)$$

The volume of runoff generated in the impluvium (Vi_{BC}) is determined by the expression:

$$V_{iBC} = Q \cdot D \cdot L \quad (15)$$

The geometric volume in the Contour Board (VBC) storage area is expressed as:

$$V_{BC} = h_{BC} \cdot D \cdot d \quad (16)$$

Where:

Q: Surface runoff generated in the implude between the contour edges in m.
D: Distance between the lateral edges, of the edge in contour, which is equal to the width of the implude in m.
L: Horizontal length of separation between edges in contour in m.

Considering the expression contribution - reception, we obtain:

$$V_{iBC} + V_{PBC} = V_{BC} + V_{INF} \quad (17)$$
$$Q \cdot D \cdot L + I_{t,T} \cdot t \cdot D \cdot d = h_{BC} \cdot D \cdot d + f_c \cdot t \cdot D \cdot d$$

From where the horizontal length (L) of separation between edges in contour, is equal to:

$$L = \frac{d \cdot \left[h_{BC} + t \cdot (f_c - I_{t.T})\right]}{Q} \quad (18)$$

The inclined length (Li) for a slope when: θ >0 is:

$$L_i = \frac{d \cdot \left[h_{BC} \cdot t \cdot (f_c - I_{t.T})\right]}{Q \cdot \cos\theta} \quad (19)$$

The application of all the methods with their respective calculation equations, allowed the dimensioning of the proposed collection systems.

3. Results

For a design rain intensity, I1.10 = 23.1 mm / h, considering a return period T = 10 years, the horizontal separation distances (L), for Half Moons and Contour Borders, with different heights of the border and water storage areas are as follows:

ISSN 2444-4987

In order to have a safety margin, it is assumed that the length calculated for pre-saturation humidity conditions (LIII), in addition to rounding to the smallest whole number, which will allow meeting the non-exceedance conditions, in both water collection systems. The magnitudes of LIII, considered in the horizontal distance, were adjusted to the slope conditions, according to equation (13), to obtain the inclined separation length (Li), allowing the correct location and implementation of the mentioned collecting measures.

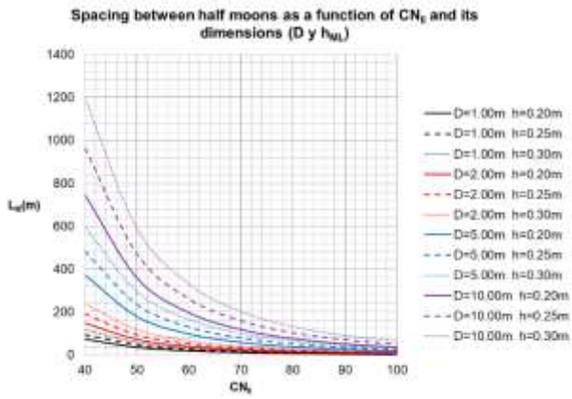

Figure 1 Spacing between half moons

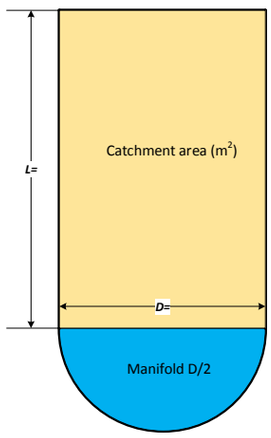

Figure 2 Catchment area between half moons

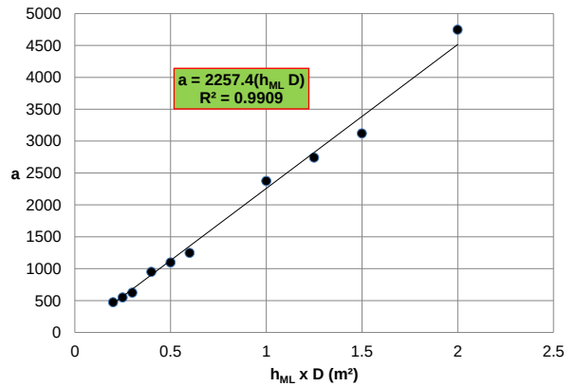

Figure 3 Ratio Coefficient 'a' - (hML x D)

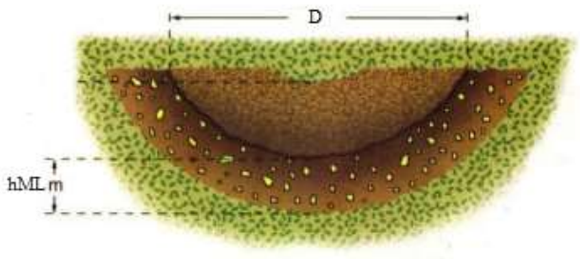

Figure 4 Plan View of (hML x D)

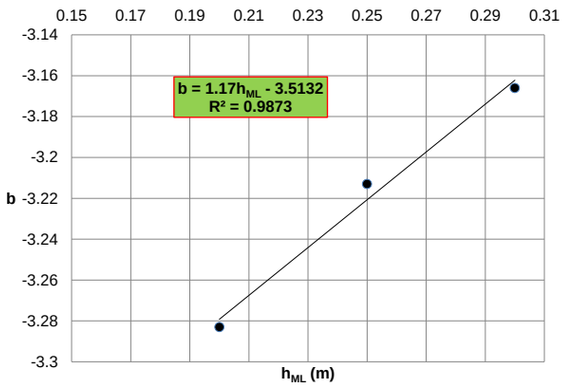

Figure 5 Coefficient 'b'- hML relationship

It can be interpreted in Figures 1,3 and 5, that the amount of surface runoff is subject to the soil conditions and characteristics of the vegetation, which define the infiltration capacity of the impluvium. This explains that, for a greater length of separation between collection systems, the soil and vegetation conditions are favorable for infiltration and water availability, the opposite being the case when there is a shorter separation distance. There is a direct relationship between the storage capacity of the collection system and the surface runoff from the impluvium. Therefore, the greater the geometric dimensions of the water storage, the greater the separation between collection systems.

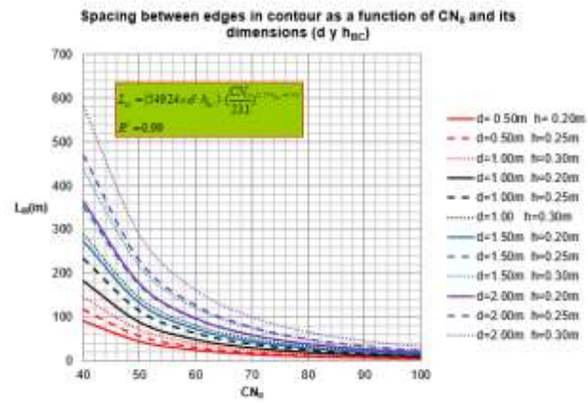

Figure 6 Edge Spacing in Contour

SCHMIDT-GOMEZ, Armando, OLIVARES-RAMÍREZ, Juan Manuel, FERRIOL-SÁNCHEZ, Fermín and MARROQUÍN-DE JESÚS, Ángel. Design of edges in contour and half moons from edaphoclimatic parameters, for the endorrheic basin of lagunas de tajzara - ramsar site 1030. Journal of Research and Development. 2021

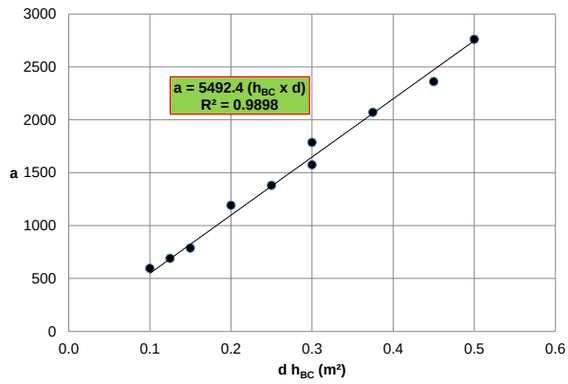

Figure 7 Ratio Coefficient 'a' - (hBC x d)

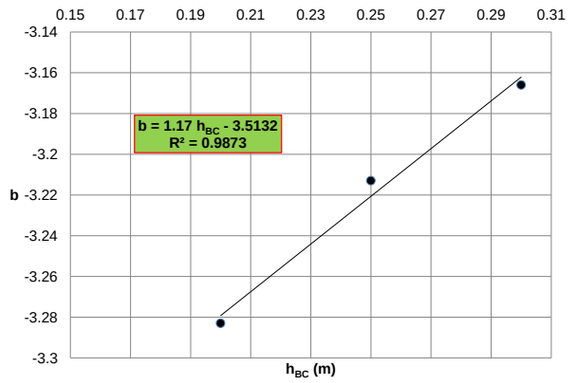

Figure 8 Relationship Coefficient 'b' - (hBC)

In the same way, it can be interpreted in Figure 6, 7 and 8, that the amount of surface runoff is conditioned to the type of soil and characteristics of the vegetation in the area, parameters that define the infiltration capacity of the impluvium. Therefore, it is explained that, for a greater length of separation between collection systems, the soil and vegetation conditions are favorable for infiltration and water availability, the opposite being the case when there is a shorter separation distance. There is a direct relationship between the storage capacity of the collection system and the surface runoff from the impluvium. In other words, the larger the geometric dimensions of the water storage, the greater the separation between collection systems.

The aforementioned is valid for all the HEUs of the basin and for the two collection systems (ML and BC), considered.

Finally, from the aforementioned relationships, the following expressions were obtained for the two water collection systems, which are expressed by the following regression equations.

a) Half Moons

$$L_{III} = \left(2257.4 \times D \cdot h_{ML}\right) \cdot \left(\frac{CN_{II}}{23.1}\right)^{(1.17 \cdot h_{ML} - 3.51)} \quad (20)$$

b) Edges in contour

$$L_{III} = \left(5492.4 \times d \cdot h_{BC}\right) \cdot \left(\frac{CN_{II}}{23.1}\right)^{(1.17 \cdot h_{BC} - 3.51)} \quad (21)$$

Where:

L_{III}: Length of separation between collection systems in m. Considering conditions of antecedent humidity in soil saturation.
D: Diameter of the Half Moons in m.
d: Length of the lateral edge in the BC system in m.
h_{ML}: Height of the ML edge in m.
h_{BC}: Height of the BC in m.
CN_{II}: Curve number for antecedent humidity condition II.

The equations described, constitute expressions of a regionalized model for the dimensioning of the collection systems, from variables of simple determination from the characterization of the site of its location. It should be noted that the regionalization is valid for all the HEUs, considering a design rainfall of 23.1 mm / h at a return period of 10 years.

Figure 9 Photograph of Ramsar Site 1030

4. Conclusions

Overgrazing in the endorheic basin of Tajzara, has caused considerable physical degradation of the soil, with the compaction of the same and the depletion of the vegetation, which, due to the reduction of infiltration and the permanent browsing of the pastures, have led to degradation in the composition of species, the reduction of protection to the soil against the impacts of raindrops, the start of particles and soil erosion, which in synergy alter the hydric flows of recharge to the water sources and wetlands of the basin.

ISSN 2444-4987

The Water Harvest, expressed by two Water Collection Systems: half-moons and Edges in Contour, constitute green infrastructure measures, which will make viable the restoration of pastures and shrubs with forage value, because before the capture and storage of surface runoff, It will increase the infiltration and the storage of the water available for the development of the plants, in addition to favoring the hydric recharge to springs, wetlands, rivers and wetlands.

For the correct operation of the water collection systems, the hydrological design must consider the criterion of "no exceedance", considering the runoff generated for maximum intensity rain events, with a return period of 10 years. The dimensions of the geometric storage of the collection system must retain runoff volumes from impluvium with adequate lengths of separation between systems, to avoid considerable environmental and landscape alterations, as well as optimizing construction and maintenance costs for Media Moons and Bordos. in Contour.

Regionalized design criteria were obtained, valid for the soil, vegetation and relief conditions that are expressed in the Curve Number (CNII), with a design rainfall of 23.1 mm / h, calculated for a return period of 10 years. which is only applicable to the twelve UEH, of the basin. The regression equations obtained (20 and 21) make it possible to estimate the separation length between collection systems and define the implude area.

For the construction of the collection systems, the construction engineers can design them, considering the geometric dimensions for the storage of water, determining the curve number, from direct observations of the conditions of the soil, vegetation and slope of the construction site, which will enable the correct execution and implementation of the systems, based on easily quantified variables.

4. References

[1] Arévalo Morán, W. V. (2021). Diseño de un mecanismo de fuerza para automatizar la siembra de arroz.

[2] Carvalho, B. M. S. A. (2021). Zoneamento Edafoclimático da Nogueira-Pecã-Carya illinoinensis, no Rio Grande do Sul–RS, Brasil (Doctoral dissertation)

[3] Farfán Loaiza, R. D. y Farfán Tenicela, E. R. (2012). Producción de pasturas cultivadas y manejo de pastos naturales alto andinos. Moquegua: INIA-Gobierno Regional de Moquegua, pp. 249. Arequipa, Perú.

[4] Flores, J. P. (2012). Diseño de zanjas de infiltración en zonas no aforadas usando SIG. Instituto Mexicano de Tecnología del Agua. Tecnología y Ciencias del Agua, vol. III, núm. 2, pp. 27-39. Morelos, México

[5] Foster, M. E.; Chen, D.; Kieser, M. S. (2020). Zanjas de infiltración. Cuantificación de beneficios potenciales en el caudal base y reducción de sedimentos. Cuantificación de Beneficios Hidrológicos de Intervenciones en Cuencas (CUBHIC). USAID, pp. 16. Canada.

[6] Francisco, P. R. M., Santos, D., Barbosa, R. B. G., Leite, N. M. G., & do Nascimento Ribeiro, G. (2021). Zoneamento agrícola de risco climático da região do Médio Curso do Rio Paraíba. Brazilian Journal of Development, 7(3)

[7] Hospital Villacorta, J.M.; Martínez de Azagra, A.; Rivas Gonzales, J.C. (2006). Determinación de Números de Curva. Programa de apoyo a MODIPE. Unidad Docente de Hidráulica e Hidrología. Universidad de Valladolid, España.

[8] Mongil, J.; Martínez de Azagra, A.; Sánchez, E. & García, M. (2009). Sistemas tradicionales de recolección de escorrentía en laderas. En: J. Navarro, A. Martínez de Azagra y J. Mongil (Coords.), Hidrología de conservación de agua. Captación de precipitaciones horizontales y de escorrentías en zonas secas. Servicio de Publicaciones Universidad de Valladolid. Valladolid, España.

[9] Mongil Manso, J. (2011). Técnicas tradicionales de recolección de agua: posibilidades de empleo en la restauración forestal. Actas de la II Reunión sobre Hidrología Forestal. Cuad. Soc. Esp. Cienc. For. 32: pp.123-128. Madrid, España.

[10] Navia, J.O. (2004). Estudio de las aguas superficiales de la reserva biológica de la cordillera de Sama. Servicio Nacional de Áreas Protegidas. Ministerio de Desarrollo Sostenible, pp. 102. Tarija, Bolivia.

ISSN 2444-4987

[11] Pizarro, R.; Flores, J.; Sangüesa, C.; Martínez, A.; García, J. (2004). Diseño de obras para la conservación de aguas y suelos. pp.146, Chile.

[12] Placido campos, S. Y., & Salvatierra Reyna, K. E. (2021). Propuesta de diseño del canal Barrio Nuevo para un sistema de riego distrito de Victor Larco-provincia Trujillo-La Libertad 2020.

[13] Perret D. S.; Wrann H. J.; Andrade V. F. (2000). Aplicación de técnicas de captación de aguas lluvia en predios de secano para forestación. Instituto Nacional Forestal. Proyecto de Desarrollo de las Comunas Pobres de Secano. Manual 25, pp. 43. Santiago de Chile.

[14] Ríos Velásquez, J.W.; Acosta Galarza, I. (1996). Evaluación de pasturas en la comunidad de Tajzara. Manejo Sostenible de Praderas Nativas Andinas, pp. 59-84. Potosí, Bolivia.

[15] Telles Antonio, R., Alanís Rodríguez, E., Jiménez Pérez, J., Aguirre Calderón, O. A., Treviño Garza, E. J., & Santos Posadas, H. M. D. L. (2021). Edaphic and topographic characteristics associated with growth in volume of Gmelina arborea Roxb, in Tlatlaya, Mexico State. Madera y bosques, 27(1)

ISSN 2444-4987

Article **Journal of Research and Development**
June, 2021 Vol.7 No.19 9-21

Active disturbance rejection control of a permanent magnet synchronous generator for wind turbine applications

Control por rechazo activo de perturbaciones de un generador síncrono de imanes permanentes para aplicaciones en aerogeneradores

AGUILAR-ORDUÑA, Mario Andrés†* & SIRA-RAMÍREZ, Hebertt José

Centro de Investigación y de Estudios Avanzados del Instituto Politécnico Nacional (CINVESTAV)

ID 1st Author: *Mario Andrés, Aguilar-Orduña* / **ORC ID:** 0000-0002-0414-3864, **CVU CONACYT ID:** 702805

ID 1st Co-author: *Hebertt José, Sira-Ramírez* / **ORC ID:** 0000-0003-0118-4764, **CVU CONACYT ID:** 20550

DOI: 10.35429/JRD.2021.19.7.9.21 Received March 27, 2021; Accepted June 30, 2021

Abstract

With sight on maximizing the amount of energy that can be extracted, by a wind turbine, from the wind, this article solves the maximum power point tracking problem for a permanent magnet synchronous generator-based horizontal wind turbine connected to the electrical grid. A three-phase back-to-back converter, which allows a decoupling between the electrical grid and the generator, is employed as an interphase between the wind turbine and the utility grid. Based on the mathematical model in the synchronous reference frame and taking advantage of the differential flatness property the system exhibits, controllers based on the active disturbance rejection methodology are designed, in this work, to track the curve of maximum extracted power from the wind and manage the generated electricity into the grid. At the same time, the phase angle of the electricity generated is synchronized with the phase angle of the electrical grid. Numerical simulations are performed to support the controllers presented in this work.

Wind Turbine, Differential flatness, ADRC

Resumen

Con vistas a maximizar la cantidad de energía que es posible extraer del viento, el presente trabajo resuelve el problema del seguimiento del punto de máxima extracción de potencia, para un aerogenerador de eje horizontal basado en un generador síncrono de imanes permanentes, conectado a la red eléctrica a través de un convertidor trifásico de potencia Back to Back, el cual permite un desacoplo entre el generador síncrono de imanes permanentes y la red eléctrica. Partiendo del modelo matemático en el marco de referencia síncrono, y explotando la propiedad de planitud diferencial que exhibe el sistema, se diseñan esquemas de control basados en la metodología del rechazo activo de perturbaciones, para realizar el seguimiento de la curva de máxima extracción de potencia y regular la energía que se suministra a la red eléctrica. Simultáneamente, se sincroniza la fase de la energía producida por el generador eléctrico con la fase de la red eléctrica. Los desarrollos presentados en este trabajo son respaldados mediante simulaciones numéricas.

Aerogenerador, Planitud diferencial, ADRC

Citation: AGUILAR-ORDUÑA, Mario Andrés & SIRA-RAMÍREZ, Hebertt José. Active disturbance rejection control of a permanent magnet synchronous generator for wind turbine applications. Journal of Research and Development. 2021. 7-19: 9-21

* Author Correspondence (mario.aguilaro@cinvestav.mx).
† Researcher contributing as first author.

Introduction

Since a long time ago, humanity has been interested in using wind power to ease or solve various tasks and even necessities, such as grain milling and water pumping. When electric power arose, engineers and researchers begin to look at wind power as a powerful energy source apt to drive electric generators. Thus, wind energy started to be used in electric power generation, emerging the first wind turbines.

Nowadays, climate change, the looming shortage of fossil fuels, a growing concern for the environment, and a diversification tendency in the electrical power industry have been driving the evolution of wind turbine technology, as it similarly happened in 1970 when the oil crisis triggered a higher interest and development of wind turbines. The evolution of this technology is such that today the renewable energy with the highest growth in the world is wind energy (Ackermann & Söder, An overview of wind energy-status 2002, 2002) (Bianchi, de Battista, & Mantz, 2007).

Various problems and research topics have arisen from the great interest and development around wind energy, most of them focused on maximizing the amount of energy extracted from the wind. Around this problem, researchers and engineers have proposed different solutions. Among others, the proposals range from the entire design of the wind turbine or even the aerodynamic profile of the blades to the electric generator selection in wind turbine construction. In this way, various wind turbine designs have arisen, some of them with fixed or variable pitch angle blades or even blades that can change their aerodynamic profile. Other wind turbine designs consider different electric generator topologies, which can work, either with a fixed or variable angular speed. All focused on extracting the maximum amount of energy from the wind (Ackermann, Wind power in power systems, 2005) (Wu, Lang, Zargari, & Kouro, 2011).

Consequently, wind turbines are becoming increasingly complex mechatronic systems, which require control designs that guarantee a safe and suitable performance of the whole system and even the interacting subsystems that compound them. Furthermore, those control designs must maximize the amount of energy extracted from the wind.

Recently permanent magnet synchronous generator (PMSG) has been the subject of great interest owing to its high efficiency, construction and, maintenance simplicity, besides its design capacity of integrating a large number of pole pairs, allowing the development of direct driven wind turbines. It's important to consider that PMSGs are not the most employed in the wind turbine market, mainly due to the high cost (which has been decreasing with the development of technology) of permanent magnets needed in their construction.

Due to the number capability of pole pairs of PMSG, direct driven wind turbines can easily prescind of those heavy and complex gearboxes employed to adjust the low angular speed of the blades to match the high angular velocity of the electric generator. The lack of a gearbox reduces the weight of the wind turbine and the number of mechanical elements which require frequent maintenance and are also a source of failures principally due to the changing nature of the wind (Polinder, et al., 2013).

The design of control schemes that maximize the amount of energy extracted from the wind by suitable and safe control of the wind turbine, despite the numerous disturbances and uncertainties that these systems are subject to, plays a relevant role in the evolution of this technology. Many control technics have been used to control wind turbines, such as gain scheduling, optimal control, sliding mode control, to mention a few (Njiri & Söffker, 2016).

This work presents control schemes based on the Active Disturbance Rejection Control (ADRC). We take advantage of the differential flatness property that the permanent magnet synchronous generator exhibits for this purpose. The maximum power point tracking (MPPT) control task of a horizontal axis wind turbine driven by a PMSG connected to the electrical grid via a three-phase back-to-back converter is solved.

In subsequent sections are presented the mathematical model of the wind turbine, followed by the problem formulation and control objectives. Later on, the differential flatness of the system is found and used to design the control schemes and solve the control objectives previously presented. Numerical simulations test and support the control schemes developed.

ISSN 2444-4987

The final sections contain the conclusions and bibliography references.

The dynamic model of a direct-driven horizontal axis wind turbine

Consider a direct-driven horizontal axis wind turbine based on a PMSG connected to the electric grid via a back-to-back converter, as shown in Figure 1. In these types of wind turbines, the blades rotor is directly coupled to a PMSG constructed with a large number of pole pairs (i.e., without a gearbox). The PMSG is connected to the grid with a Back-to-Back converter.

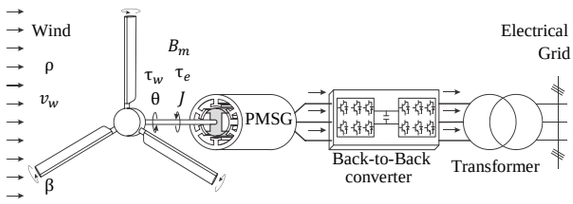

Figure 1 Direct-driven horizontal wind turbine based on a PMSG
Source: Made by the author

To model the system, we divide the wind turbine into three principal subsystems, the blades, the permanent magnet synchronous generator and, the grid side converter which, couples the wind turbine with the electrical grid.

Wind energy extraction

The blades of a wind turbine are the elements that transform the kinetic energy in the wind into mechanical energy. The power that blades extract from the wind is given by,

$$P_w = \frac{1}{2}\rho A v_w^3 C_p(\lambda_t, \beta) \quad (1)$$

Where ρ is the air density, $A = \pi r_t^2$ is the area cover by the rotor blades with a radius r_t, v_w is the wind speed and, C_p is a power coefficient dependent on the blade aerodynamic design; it's important to say that C_p is bounded by 0.593, known as the Betz limit. This power coefficient is a function of the blades pitch angle β and the tip speed ratio λ_t defined as:

$$\lambda_t = \frac{\omega_t r_t}{v_w} \quad (2)$$

With ω_t is the rotor's angular velocity. The shaft mechanical torque produced by the wind is given by the equation:

$$\tau_w = \frac{P_w}{\omega_t} = \frac{1}{2}\rho\pi r_t^3 v_w^2 \frac{C_p(\lambda_t,\beta)}{\lambda_t} \quad (3)$$

As we are working with a direct-driven wind turbine, the mechanical equation of the system corresponds to the equation of a single rotating mass:

$$J\ddot{\theta} + B\dot{\theta} + \tau_e = \tau_w \quad (4)$$

Where $\frac{d}{dt}\theta = \dot{\theta} = \omega_t, \frac{d^2}{d^2t}\theta = \ddot{\theta}$ and θare the systems velocity, acceleration, and angular position respectively; J is the inertia momentum of the whole system, B is the systems friction coefficient and τ_e is the electromagnetic torque of the PMSG.

Permanent magnet synchronous generator model

Consider a round rotor PMSG with sinusoidal flux permanent magnets. It's supposed a star connection in PMSG windings, see Figure 2.

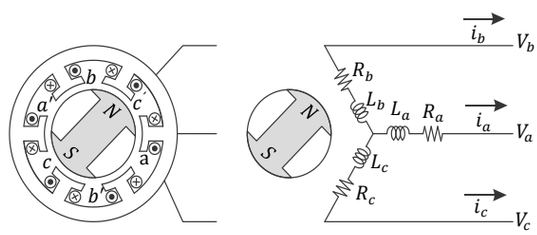

Figure 2 Permanent magnet synchronous generator
Source: Made by the author

While we are working with a synchronous machine, the inductances and resistors of the different windings are all nearly of the same value. The dynamic model of the permanent magnet synchronous generator is obtained, in the synchronous (d-q) reference frame, by employing the Clark and Park transformations into the machine electrical equations in the natural (a-b-c) reference frame. By selecting $\theta_p = n_p\theta$ as the Park angle, the model is:

$$v_d = R_s i_d - \frac{3}{2}L_s i_q n_p \frac{d}{dt}\theta + \frac{3}{2}L_s \frac{d}{dt} i_d \quad (5)$$

$$v_q = R_s i_q + \frac{3}{2}L_s i_d n_p \frac{d}{dt}\theta + \frac{3}{2}\kappa\lambda_0 n_p \frac{d}{dt}\theta + \frac{3}{2}L_s \frac{d}{dt} i_q \quad (6)$$

$$\tau_e^{dq} = \frac{n_p \lambda_0}{\kappa} i_q = k_m i_q \quad (7)$$

Where R_s and L_s are the stator inductance and resistance, respectively, n_p is the number of pole pairs, κ is a Clark transformation scaling factor, andλ_0 is the electromagnetic flux linkages magnitude. The currents i_d and i_q, are the synchronous reference frame electrical currents and, v_d, v_q, are their respective voltages, which are the system control inputs. A three-phase Back-to-Back converter induces those voltages into the PMSG; this work considers the average model of the three-phase Back-to-Back converter. Notice that the angle θ represents the angular displacement of both the permanent magnet synchronous generator and the wind turbine's rotor since we consider a direct-driven wind turbine.

Model of the grid side converter

The Back-to-Back converter DC-link and the filter that connects the wind turbine with the electrical grid constitutes the grid side converter (GSC). See Figure 3.

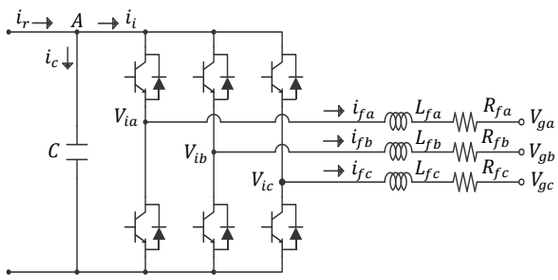

Figure 3: Grid Side Converter with an RL filter
Source: Made by the author

Since we are working with a three-phase balanced system, each filter-branch inductance and resistance must have the same value. And supposing a lossless DC-link, whose voltage is given by,

$$\frac{d}{dt} V_{dc} = \frac{1}{C} i_c = \frac{1}{C} (i_r - i_i) \quad (8)$$

By taking the integral of the electrical grid frequency as Parks angle, i.e., $\theta_p = \int \omega_p$, the dynamic model in the synchronous reference frame of the grid side converter is:

$$V_{id} = R_f i_{fd} - L_f i_{fq} + L_f \frac{d}{dt} i_{fd} + V_{gd} \quad (9)$$

$$V_{iq} = R_f i_{fq} + \omega_p L_f i_{fd} + L_f \frac{d}{dt} i_{fq} + V_{gq} \quad (10)$$

The instantaneous active power P and reactive power Q that the system exchanges with the electrical grid, usually defined in the fixed reference frame $\alpha - \beta$ (Akagi, Watanabe, & Aredes, 2017), can be expressed via the Park transformation in the synchronous reference frame as,

$$P = \frac{3}{2} \left(V_{gd} i_{fd} + V_{gq} i_{fq} \right) \quad (11)$$

$$Q = \frac{3}{2} \left(V_{gq} i_{fd} - V_{gd} i_{fq} \right) \quad (12)$$

By equating the DC-link power with the instantaneous active power and, considering that the grid is a balanced three-phase system (notice that in this case, the voltage $V_{gq} = 0$), we obtain the following expressions for the active and reactive instantaneous powers:

$$P = \frac{3}{2} V_{gd} i_{fd} = V_{cd} i_i \quad (13)$$

$$Q = -\frac{3}{2} V_{gd} i_{fq} \quad (14)$$

Problem formulation and control objectives

The main objective of a wind turbine is the wind's kinetic energy conversion into electrical power. Figure 4 shows four wind-speed dependant work zones where different generation objectives are defined.

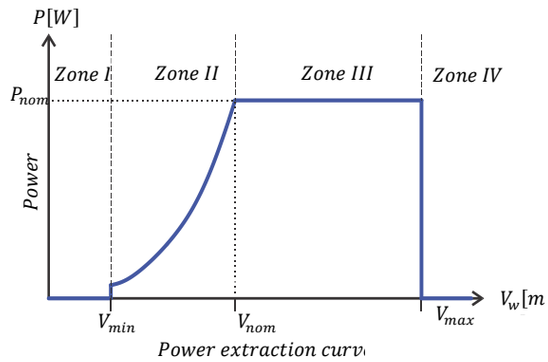

Figure 4 Wind-speed dependent work zones.
Source: Made by the author

Zone I occur when the wind speed is less than the cut-in wind speed, i.e., $v_w < v_{min}$. In this zone, the wind energy is too low to overcome the friction forces and the system's inertia.

In Zone IV, the wind speed exceeds the wind turbine's maximum wind speed limit for a safe operation, i.e., $v_w > v_{max}$. Hence the wind turbine must be stoped to avoid damage or a possible failure of the system. So, in Zones I and IV, it is impossible to extract energy from wind.

At Zone III ($v_{nom} < v_w < v_{max}$), the electric generator must operate at its nominal velocity, so the blades' pitch-angles β are adjusted to limit the power extracted from the wind and hence the rotors' angular speed and avoid overcharge.

Zone II corresponds to wind speeds between the cut-in and nominal wind velocity, i.e. ($v_{min} < v_w < v_{nom}$). At this zone, the wind energy is enough to move the wind turbine, but it's not enough to speed up the generator at its nominal speed. Therefore, the generation objective in zone II is to maximize the energy extracted from the wind by adjusting the blades' pitch angle towards $\beta = 0$; however, this is not enough while the power coefficient C_p is also tip speed ratio dependant. If we can control the angular velocity of the electric generator, then we can regulate the tip speed ratio to an optimal point. And thus extract the maximum amount of energy from the wind. Figure 5 depicts the so-called maximum power curve.

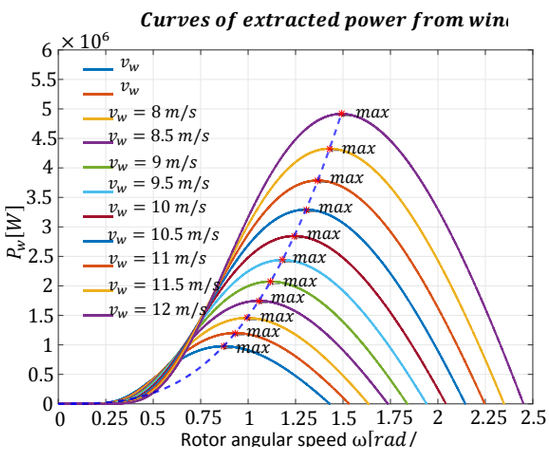

Figure 5 Maximum power curve plot.
Source: Made by the author

The above-mentioned reveals the first control objective that is the maximum power curve tracking (MPPT). For this, the desired velocity reference is given by,

$$\omega_{t,opt}^{*} = \dot{\theta}_{opt} = \frac{\lambda_{t,opt} v_w}{r_t} \tag{15}$$

where $\lambda_{t,opt}$ is the optimum tip speed ratio obtained from the graphs of the power coefficient by setting $\beta = 0$. The reference signal is passed through a low pass filter to eliminate the influence of the turbulence and thus avoid excessive stress into the PMSG. From the electric power equation of the PMSG, we can find the term $R_s(i_d^2 + i_q^2)$, which refers to Joule's losses commonly manifested as heat in the machine. The second control objective is to regulate the current $i_d = 0$ and thus minimize Joule's losses.

The signals induced by the Back-to-Back converter to either the permanent magnet synchronous generator and the grid filter need an adequate DC-link Voltage. Also, a desirable DC-link voltage is required to inject the PMSG active power into the electrical grid. Therefore, the third control objective is to regulate the DC-link Voltage V_{dc} toward the desired value V_{dc}^{*}.

One of the advantages of employing a Back-to-Back converter is the reactive power regulation capacity, allowing the control of the absorbed or supplied reactive power to the electrical grid. So the fourth control objective is to regulate the reactive power Q towards a reference value Q^{*}. Finally, to supply the energy into the electrical grid, the electricity generated by the wind turbine must be synchronized with the electricity in the grid. So the fifth control objective is the synchronization of the electricity between both systems.

Differential flatness

Differential flatness is a property of dynamic systems that allows parametrizing all system variables (i.e., states, inputs, and outputs) into algebraic-differential expressions in terms of a finite set of independent special-outputs, called flat-outputs. If the above-mentioned happens, the system is called differentially flat. Fliess and his collaborators first introduced this property in (Fliess, Lévine, Martin, & Rouchon, 1992).

The differential flatness property is tightly related to the feedback linearization, controllability and, observability concepts. This property trivializes the trajectory planning and is often employed as a tool for analysis purposes of relevant system properties, such as parametrization of the equilibrium point, minimum and non-minimum properties, among others.

It is possible to take advantage of the flatness property and combine it with control schemes such as passivity, optimal control, sliding mode control, active disturbance rejection control, to mention a few (Sira-Ramírez & Agrawal, Differentially flat systems, 2004).

Differential flatness of the wind turbine

The dynamic model of the PMSG in equations (4), (5), (6), and (7) in conjunction with equations (10) and (10) corresponding to the GSC dynamic model, compound the dynamic model of the wind turbine. Notice the four control inputs v_d, v_q, V_{id}, and V_{iq} of the system. Therefore, we expect to obtain four flat outputs. By inspecting the PMSG equations, we can observe that the control inputs, equations (5) and (6), and the phase variables are parametrizable in terms of the current i_d, the angular position θ, and their respective derivatives.

$$\frac{d}{dt}i_d = \left(\frac{2}{3L_s}\right)\left(v_d - R_s i_d - \frac{3}{2}L_s i_q n_p \frac{d}{dt}\theta\right) \quad (16)$$

$$\frac{d}{dt}i_q = \left[\frac{2}{3L_s}\right]\left[v_q - R_s i_q - n_p \frac{d}{dt}\theta\left(\frac{3}{2}L_s i_d + \frac{3}{2}\kappa\lambda_0\right)\right] \quad (17)$$

$$\frac{d^2}{d^2t}\theta = \left(\frac{1}{J}\right)\left(\tau_w - B_m \frac{d}{dt}\theta - \frac{n_p\lambda_0}{\kappa} i_q\right) \quad (18)$$

$$i_q = \left(\frac{\kappa}{n_p\lambda_0}\right)\left(J\frac{d^2}{d^2t}\theta - \tau_w + B_m \frac{d}{dt}\theta\right) \quad (19)$$

Thus, the current i_d and the angular position θ qualifies as the first two flat outputs of the system.

Now, notice that from the grid side converter equations and by employing the relations in (13) and (14), we obtain the following expressions for the phase variables,

$$I_{fq} = -\frac{2}{3V_{gd}}Q \quad (20)$$

$$I_{fd} = \frac{2V_{cd}}{3V_{gd}}\left(I_r - C\frac{d}{dt}V_{cd}\right) \quad (21)$$

Which are expressed in terms of the reactive power Q and the DC-link voltage V_{cd}. The same happens with the control inputs in equations (10) and (10). Therefore, Q and V_{cd} qualifies as the second pair of flat-outputs of the system, completing the four expected flat-outputs.

By deriving each one of the flat outputs, we obtain the dynamic model of the PMSG in input-output form as,

$$\theta^{(3)} = -\left(\frac{n_p\lambda_0}{JL_s}\right)v_q + \left(\frac{1}{J}\right)\dot{\tau}_m\left(\frac{n_p\lambda_0}{JL_s}\right) - \left(R_s i_q + \frac{3}{2}n_p\dot{\theta}(L_s i_d + \kappa\lambda_0) + B_m\ddot{\theta}\right) \quad (22)$$

$$\frac{d}{dt}i_d = \left(\frac{2}{3L_s}\right)v_d + \left(\frac{2}{3L_s}\right)\left(-R_s i_d - \frac{3}{2}L_s i_q n_p \frac{d}{dt}\theta\right) \quad (23)$$

And for the GSC we have

$$\ddot{V}_{cd} = -\frac{3V_{gd}}{2L_f V_{dc}}V_{id} - \frac{3V_{gd}}{2V_{dc}}\left(-V_{gd} - R_f I_{fd} + \omega_p L_f I_{fq}\right) + \frac{\dot{I}_r}{C} - \frac{3\dot{V}_{gd}I_{fd}}{2V_{cd}} + \frac{3V_{gd}I_{fd}\dot{V}_{cd}}{2V_{cd}^2} \quad (24)$$

$$\dot{Q} = -\frac{3V_{gd}}{2L_f}V_{iq} - \frac{3V_{gd}}{2}\left(-V_{gq} - R_f I_{fq} - \omega_p L_f I_{fd}\right) - \frac{3}{2}\dot{V}_{gd}I_{fq} \quad (25)$$

Active disturbance rejection control.

Active disturbance rejection control is a robust control technic, whose main idea is to simplify the description of the system by groping in a time-varying total disturbance term all endogenous and exogenous disturbances affecting the system. For example, the disturbance term can contain unmodeled dynamics, parameters uncertainties, and external influences. Further, the effect of the total disturbance term over the system is estimated and canceled as part of a feedback control law.

Usually, the control law employed in the ADRC scheme requires complete access to all phase variables. Unfortunately, this knowledge is not always available. Commonly, the design of a suitably extended state observer (ESO) or a reduced-order extended state observer (ROESO) is employed to estimate the phase variables and even the influence of the total disturbance term. Then, a feedback control law is design under the basis of those estimations and subtracting the estimate of the disturbance term to solve the entrusted control task (Sira-Ramírez, Luviano-Juárez, Ramírez-Neria, & Zurita-Bustamante, 2017).

Permanent magnet synchronous generator angular speed control

Following the active disturbance rejection methodology, lets consider the input-output model in equation (22), written in simplified form:

$$\theta^{(3)} = -\left(\frac{n_p\lambda_0}{JL_s}\right)v_q + \xi_\theta = U_q + \xi_\theta \qquad (26)$$

Where $U_q = -\left(\frac{n_p\lambda_0}{JL_s}\right)v_q$ is the control input and $\xi_\theta = \left(\frac{1}{J}\right)\dot{\tau}_m\left(\frac{n_p\lambda_0}{JL_s}\right) - \left(R_s i_q + \frac{3}{2}n_p\dot{\theta}(L_s i_d + \kappa\lambda_0) + B_m\ddot{\theta}\right)$ the total disturbance term. Writing the simplified system in terms of the tracking error we get,

$$e_\theta^{(3)} = e_{U_q} + \xi_\theta \qquad (27)$$

Where the tracking error of the angular displacement is$e_\theta = \theta - \theta^*$ and the control input error is $e_{U_q} = U_q - U_q^*$ with $\theta^* = \int \dot{\theta}_{opt}$ and $U_q^* = \frac{d^3}{dt^3}\theta^*$.

It's worth saying that we suppose that only the control input and the angular position are available for measurement. Thus an extended state observer is designed to estimate the disturbance and the non-measured states. Let's define $e_\theta = e_{y_0}, \dot{e}_\theta = e_{y_1}, and\ \ \ddot{e}_\theta = e_{y_2}$ so

$$\begin{aligned}
\dot{\hat{e}}_{y_0} &= \widehat{e_{y_1}} + \lambda_3\left(e_{y_0} - \widehat{e_{y_0}}\right) = \widehat{e_{y_1}} + \lambda_3\widetilde{e_0}\\
\dot{\hat{e}}_{y_1} &= \widehat{e_{y_2}} + \lambda_2\widetilde{e_0}\\
\dot{\hat{e}}_{y_2} &= e_{U_q} + z + \lambda_1\widetilde{e_0}\\
\dot{z} &= \lambda_0\widetilde{e_o}
\end{aligned} \qquad (28)$$

The terms $\widehat{e_{y_x}}$ represents the state error estimations, and z is the total disturbance term estimation. Then, the observer errors are defined by

$$\begin{aligned}
\widetilde{e_0} &= e_{y_0} - \widehat{e_{y_0}}\\
\widetilde{e_1} &= e_{y_1} - \widehat{e_{y_1}}\\
\widetilde{e_2} &= e_{y_2} - \widehat{e_{y_2}}\\
\zeta_e &= \xi_\theta - z
\end{aligned} \qquad (29)$$

Whose dynamics satisfy the following differential equation. By defining $e_0^{(x)} = \frac{d^x}{dt^x}e_0$ we have

$$\widetilde{e_0^{(4)}} + \lambda_3\widetilde{e_0^{(3)}} + \lambda_2\widetilde{e_0^{(2)}} + \lambda_1\widetilde{e_0^{(1)}} + \lambda_0\widetilde{e_0} = \dot{\xi}_\theta \qquad (30)$$

The corresponding characteristic polynomial is

$$s^4 + \lambda_3 s^3 + \lambda_2 s^2 + \lambda_1 s + \lambda_0 = 0 \qquad (31)$$

From where, we can observe that to ensure exponential stability of the observer, the set of gain parameters $\lambda_3, \lambda_2, \lambda_1, \lambda_0$ must compound a Hurwitz set. For that reason, the gain parameters are computed as:

$$\begin{aligned}
\lambda_0 &= \omega_n^4\\
\lambda_1 &= 4\zeta\omega_n^3\\
\lambda_2 &= 4\zeta^2\omega_n^2 + 2\omega_n^2\\
\lambda_3 &= 4\zeta\omega_n
\end{aligned} \qquad (32)$$

Where the terms $\omega_n > 0$ and $0 < \zeta < 1$ are the design parameters of the observer.

Once we computed the phase variables and the total disturbance term estimations, we propose a state estimation-based feedback controller with an additional parameter (the estimate of the total disturbance term) to cancel the influence of the total disturbance term.

$$U_q = U_q^* - k_2\hat{e}_y^{(2)} - k_1\hat{e}_y^{(1)} - k_0 e_y - z \qquad (33)$$

The characteristic polynomial obtained from the closed-loop system is

$$s^3 + k_2 s^2 + k_1 s + k_0 = 0 \qquad (34)$$

Once again, notice that the proper selection of the gain parameters $k_2, k_2\ y\ k_0$ guarantees the exponential stability of the controller. The gain parameters must compound a Hurwitz set, for that reason the gain parameters are computed as:

$$\begin{aligned} k_0 &= p\omega_n^2 \\ k_1 &= 2\zeta\omega_n p + \omega_n^2 \\ k_2 &= 2\zeta\omega_n + p \end{aligned} \tag{35}$$

The terms $\omega_n > 0, p > 0$ and $0 < \zeta < 1$ constitute the controller gain parameters.

Current i_d controller

According to the ADRC methodology, we simplify equation (23) corresponding to the PMSG input-output model for the electric current i_d,

$$\frac{d}{dt} i_d = \left(\frac{2}{3L_s}\right) v_d + \xi_{id} = U_d + \xi_{i_d} \tag{36}$$

Where $U_d = \left(\frac{2}{3L_s}\right) v_d$ is the system control input, and $\xi_{id} = \left(\frac{2}{3L_s}\right)\left(-R_s i_d - \frac{3}{2} L_s i_q n_p \frac{d}{dt}\theta\right)$ is the total disturbance term.

We use the simplified model, in equation (36), to design a proportional-integral (PI) controller to regulate the value of the current i_d towards $i_d = 0$. This controller written in a classical compensation network form is

$$U_d(s) = -\left[k_1 + \frac{k_0}{s}\right] i_d(s) \tag{37}$$

The coefficient $k_1\ and\ k_0$ are design parameters which are computed as following: ${k_0 = \omega_n}^2$ and $k_1 = 2\zeta\omega_n$ to ensure exponential stability of the controller, where ζ and ω_n must satisfy $\omega_n > 0$ y $0 < \zeta < 1$.

In recent works, it has been demonstrated that the well-known proportional integral derivative controller (PID) and flat filter controllers are equivalent to the active disturbance rejection control. See (Sira-Ramirez, Zurita-Bustamante, & Huang, 2019), (Sira-Ramírez & Zurita-Bustamante, On the equivalence between ADRC and Flat Filter based controllers: A frequency domain approach, 2021).

Sinchronization with the electrical grid

To achieve an adequate connection between the wind turbine and the electrical grid, the electricity generated by the wind turbine must be synchronized with the electricity in the electrical grid. The synchronization is not necessary only to make the connection; both systems need to be synchronized all the time. Therefore, before continuing with the control of the grid side converter, we must know or estimate the phase angle of the electrical grid. Both systems are synchronized via a phase lock loop (PLL), specifically a phase lock loop in the synchronous reference frame (SRF-PLL), which estimates the grid's phase angle. Then, the Park transformation and its inverse employ this estimate. By doing this, the controllers of the grid side converter commute the Back-to-Back converter to generate electric power in phase with the electricity in the grid. Let's suppose that the electrical grid has a cosine based function,

$$\begin{bmatrix} Vga \\ Vgb \\ Vgc \end{bmatrix} = \begin{bmatrix} V\cos(\theta_g) \\ V\cos\left(\theta_g - \frac{2\pi}{3}\right) \\ V\cos\left(\theta_g + \frac{2\pi}{3}\right) \end{bmatrix} \tag{38}$$

Where $\theta_g = \omega_g t + \phi_g$, ω_g is the grid's base frequency and ϕ_g is a deviation of the input frequency nominal value. The corresponding grid voltages in the synchronous reference frame are computed using the Clarke and Park transformations:

$$\begin{bmatrix} Vgd \\ Vgq \\ Vg0 \end{bmatrix} = \kappa \begin{bmatrix} \frac{3}{2} V\cos(\theta_g - \phi_p) \\ \frac{3}{2} V\sin(\theta_g - \phi_p) \\ 0 \end{bmatrix} \tag{39}$$

Where ϕ_p is the estimate Park's angle. Notice that if the estimate Park's angle coincides with that for the electrical grid (i.e. $\phi_p = \theta_g$), the voltage $V_{gq} = 0$. It follows that regulating the voltage V_{gq} towards zero, the electrical grid phase angle can be estimated; this is accomplished via a PI controller, as shown in Figure 6.

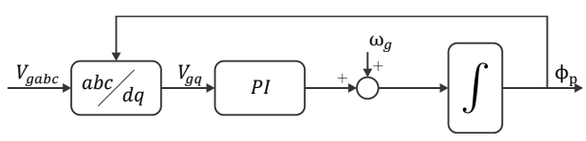

Figure 6 Synchronous reference frame phase lock loop. *Source: Made by the author*

The whole scheme is known as a phase lock loop in the synchronous reference frame (SRF-PLL). In the book (Karimi-Ghartemani, 2014), this and other topologies are presented.

DC-link voltage control

To design the control scheme that regulates the DC-link voltage towards the desired value, consider the simplified model of the equation (24),

$$\ddot{V}_{cd} = -\frac{3V_{gd}}{2L_f V_{dc}} V_{id} + \xi_{cd} = U_{id} + \xi_{cd} \qquad (40)$$

Where $U_{id} = -\frac{3V_{gd}}{2L_f V_{dc}} V_{id}$ is the control input and the total disturbance term is given by: $\xi_{cd} = -\frac{3V_{gd}}{2V_{dc}}\left(-V_{gd} - R_f I_{fd} + \omega_p L_f I_{fq}\right) + \frac{I_r}{C} - \frac{3\dot{V}_{gd} I_{fd}}{2V_{cd}} + \frac{3V_{gd} I_{fd} \dot{V}_{cd}}{2V_{cd}^2}$.

In terms of the tracking error, the simplified system is:

$$\ddot{e}_{V_{cd}} = e_{U_{id}} + \xi_{cd} \qquad (41)$$

The DC-link voltage error is $e_{V_{cd}} = V_{cd} - V_{cd}^*$ similarly, the control input error is defined as $e_{U_{id}} = U_{id} - U_{id}^*$ where V_{cd}^* is the desired value of the DC-link voltage and $U_{id}^* = \frac{d^2}{dt^2} V_{cd}^*$ is the nominal control input.

From the error simplified model, we propose the following Flat Filter controller,

$$U_{id}(s) = U_{id}^* - \left[\frac{k_2 s^2 + k_1 s + k_0}{s(s+k_3)}\right] e_{V_{cd}}(s) \qquad (42)$$

Whose characteristic polynomial is just

$$s^4 + k_3 s^3 + k_2 s^2 + k_1 s + k_0 = 0 \qquad (43)$$

As happened in the previous cases, selecting the values of gain parameters $k_3, k_2, k_1\, y\, k_0$, such that they constitute a Hurwitz set guarantees exponential stability of the controller. So, the flat Filter parameters in equation (42) are computed as in (32). It's worth mentioning that the values of these two sets of gain parameters are not necessarily the same.

Similar to the equivalence between PID and ADRC, active disturbance rejection control is also equivalent with flat filters under a co-primeness condition between the characteristic polynomials of the controller and that of the observer. So by respecting the separation principle of the observer and controller characteristic polynomials given an ADRC, we can find an equivalent flat filter (Sira-Ramírez & Zurita-Bustamante, On the equivalence between ADRC and Flat Filter based controllers: A frequency domain approach, 2021), (Sira-Ramírez, From flatness, GPI observers, GPI control and flat filters to observer-based ADRC., 2018).

Reactive power control

Following ADRC methodology, the simplified model of equation (25) is,

$$\dot{Q} = -\frac{3V_{gd}}{2L_f} V_{iq} + \xi_Q = U_{iQ} + \xi_Q \qquad (44)$$

Where the control input of the system is $U_{iQ} = -\frac{3V_{gd}}{2L_f} V_{iq}$ and the total disturbace term is given by $\xi_Q = \left(-V_{gq} - R_f I_{fq} - \omega_p L_f I_{fd}\right) - \frac{3}{2}\dot{V}_{gd} I_{fq}$.

Similar to the design of the i_d current regulation controller in previous sections, we propose a PI controller to regulate the reactive power Q to the desired value. Once again, the controller in classical compensation network form is:

$$e_{U_{iq}}(s) = -\left[k_1 + \frac{k_0}{s}\right] e_Q(s) \qquad (45)$$

Where the instantaneous reactive power error is $e_Q = Q - Q^*$ and the control input error is defined as $e_{U_{iq}} = U_{iq} - U_{iq}^*$ where Q^* is the reactive power desired value . The nominal control input is just $U_{iq}^* = \frac{d^2}{dt^2} Q^*$.

The coefficientsk_1 and k_0 are the design parameters and are computed as: $k_0 = \omega_n{}^2$ and $k_1 = 2\zeta\omega_n$ to be a Hurwitz set and thus guarantee asymptotic stability of the controller, where $\omega_n > 0$ and $0 < \zeta < 1$.

Numerical simulations

We realized numerical simulations using the software Simulink Matlab to test the performance of the previously proposed controllers. We consider a horizontal direct-driven wind turbine based on a permanent magnet synchronous generator with a power capacity of 5 MW, whose parameters are in Table 1.

.

Parameter	Symbol	Value	Unit
Nominal Power	$P_{w,nom}$	5	MW
Total inertia	J	1×10^4	$Kg \cdot m^2$
Blade length	r_t	56	m
Wind density	P	1.225	$Kg \cdot m^3$
Stator resistance	R_s	6.25	mΩ
Stator inductance	L_s	4.229	mH
Permanent magnet flux density	λ_0	11.1464	Wb
Pole pairs number	n_p	75	–
Nominal voltage	V_{nom}	0.9	kV
Nominal angular speed	ω_{nom}	1.447	rad/s

Table 1 : Wind turbine parameters
Source: (Aimene, Payman, & Dakyo, 2014)

For the connection between the wind turbine with the electrical grid, an RL filter is employed. Table 2 presents the parameters of the filter simulated. It is supposed a 0.9 kV at 60 Hz electrical grid.

Parameter	Symbol	Value	Unit
DC-Link capacitor	C	40	μF
Filter resistance	R_f	0.01	$m\Omega$
Filter inductance	L_f	0.5	mH

Table 2: Grid Side Converter parameters
Source: (Aimene, Payman, & Dakyo, 2014)

We simulate a realistic wind profile using the library "Aerospace Blockset". The wind profile has an average speed of 11 m/s, turbulence components, and wind gust characteristics. Effects that usually affect wind turbines. See Figure 7

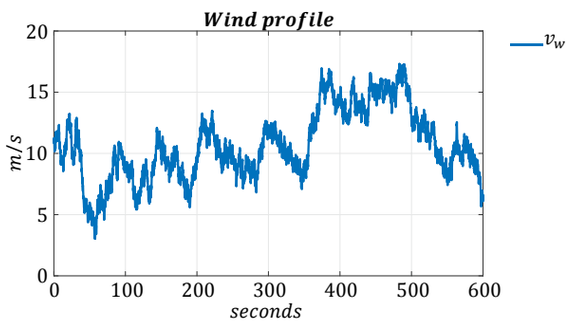

Figure 7 Simulation of a realistic wind profile
Source: Made by the author

Figure 8 shows the performance of the optimum-angular velocity tracking task, the currents i_d and i_q, the control signals, and the angular velocity and current tracking errors. Notice that the controller tracks the optimum-angular velocity with a maximum error of $1 \times 10^{-3}\ rad/s$.

Therefore, we can affirm that the ADRC controller accurately tracks the reference signal. The current i_d is close to zero, with an error of less than $0.01\ A$. The control objectives are achieved despite the presence of turbulence and wind gust effects.

Regarding the angular velocity graph, it is evident that the optimal velocity never crosses the PMGS nominal angular speed, with a value of $1.447\ rad/s$. When the wind speed exceeds its nominal value, typically, a PI controller changes the blades' pitch angle β to limit the wind energy conversion by reducing the power coefficient C_p value. In consequence, the PMSG angular speed is reduced by this effect. A PI controller for a variable speed wind turbine is presented in (Hwas & Katebi, 2012). Nevertheless, this controller is out of the scope of the current work and is left for further work.

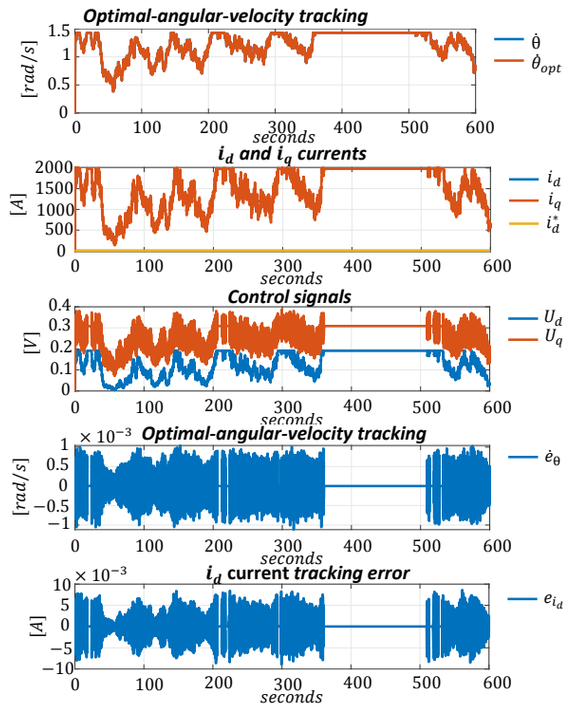

Figure 8 Angular speed, electrical currents, and control inputs for the PMSG
Source: Made by the author

Figure 9 depicts a zoom at the first ten seconds of the system operation, revealing how the system starts. It's important to say that a smooth trajectory is employed to start the system and avoid subjecting the system to excessive forces and stress. Due to we suppose that the wind turbine is in complete rest at the beginning.

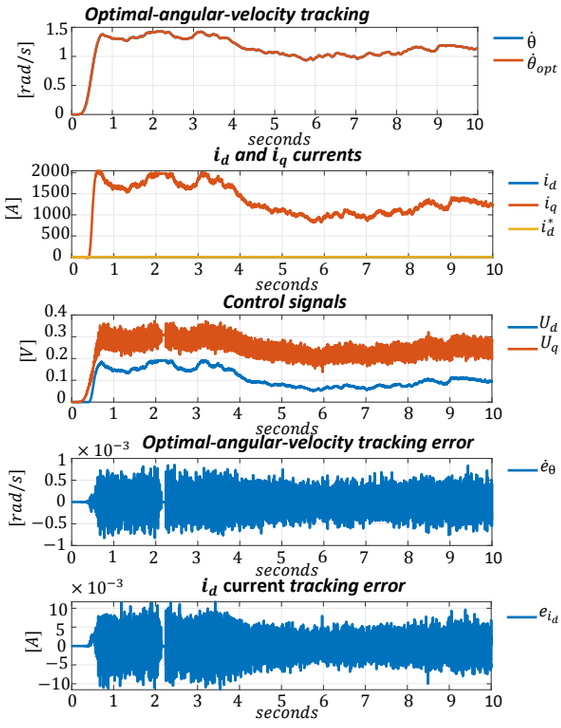

Figure 9 Angular speed and electrical currents during wind turbine startup
Source: Made by the author

Figure 10 presents the graphs obtained for the behavior of the grid side converter. The proposed controller maintains the DC-link voltage in its reference value, $4700\ V$. Also, the PI controller tracks the desired reference, which represents the reactive power supplied or absorbed from the electrical grid. Notice that once the wind turbine reaches approximately an angular speed of $0.35\ rad/seg$, the PMSG starts to generate electrical power, and the filter currents start to rise. The magnitude of the filter electric currents varies according to the wind speed.

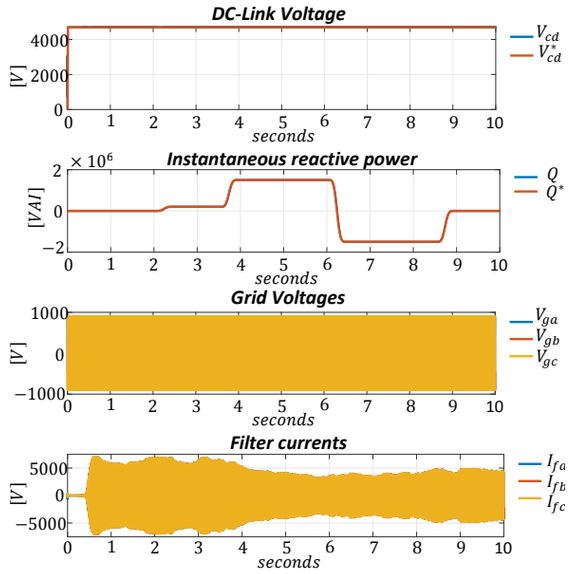

Figure 10: DC-link voltage and instantaneous active and reactive power. Source: Made by the author.

Zooming one more time from $t = 1[s]$ to $t = 1.1[s]$, see Figure 11 notice the approximately $10[V]$ variation in the DC-link voltage. The DC-link voltage is constantly subject to voltage variations due to the repeated charge and discharge of the capacitor, caused by the changes in wind speed, thus the PMSG angular velocity, and the management of the electrical energy supply to the grid.

Despite all the above, the proposed controller achieves a DC-Link voltage so close to the desired reference by the proper commutation of the grid side converter. It is also noticed that the value of the instantaneous reactive power highly approaches its reference value.

Finally, notice that the current supplied to the electrical grid is synchronized and has a 60 Hz frequency.

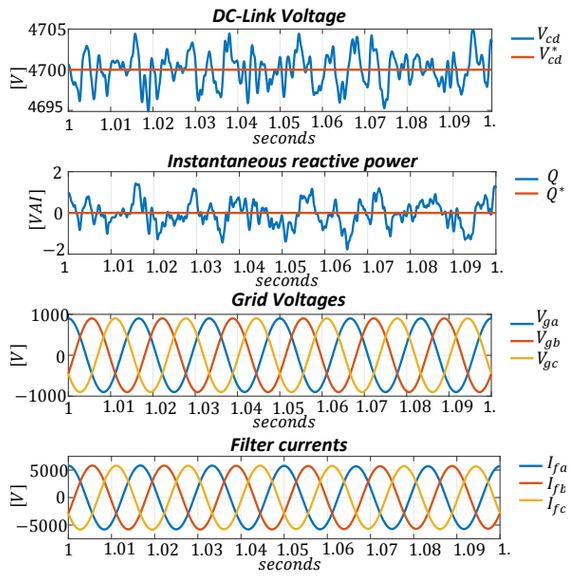

Figure 11: Zoom to grid voltages and filter currents. *Source: Made by the autho*

Conclusions

The main objective of this manuscript is to take advantage of the PMSG differential flatness property and employ robust control strategies to solve the MPPT control problem and manage the electricity generated to the electrical grid considering a horizontal axis wind turbine with a PMSG connected to the grid.

The flatness property and the control schemes employed in this work give the advantage of avoiding measuring the complete state of the system also offer a good performance despite unknown dynamics, unknown parameters, and external disturbances. Despite the subsystems that compound the wind turbine interacts with each other, this methodology allows designing control schemes for each system independently.

Numerical simulations show that the active disturbances rejection controller offers good performance, even when the control design is done under a quite simplified model of the system and despite all the disturbances affecting the system and the nonlinearities ignored.

In further work, we pretend to design control schemes to solve the maximum power point tracking without the measurement of the angular position of the permanent magnet synchronous generator and even avoiding the measurement of wind speed to reduce cost or improve the performance of the whole system.

References

Ackermann, T. (2005). *Wind power in power systems.* Chichester, UK: John Wiley.

Ackermann, T., & Söder, L. (2002). An overview of wind energy-status 2002. *Renewable and Sustainable Energy Reviews*, 67-127.

Aimene, M., Payman, A., & Dakyo, B. (2014). Flatness-based control of a variable-speed wind-energy system connected to the grid. *Ninth International Conference on Ecological Vehicles and Renewable Energies*, (pp. 1-7). Monte-Carlo, Monaco.

Akagi, H., Watanabe, E. H., & Aredes, M. (2017). *Instantaneous power theory and applications to power conditioning.* Hoboken, New Jersey: John Wiley & Sons.

Bianchi, F. D., de Battista, H., & Mantz, R. J. (2007). *Wind Turbine Control Systems.* London: Springer-Verlag.

Fliess, M., Lévine, J., Martin, P., & Rouchon, P. (1992). Sur les systèmes non linéaires différentiellement plats. *CR Acad. Sci.*, (pp. 619-624). Paris.

Hwas, A., & Katebi, R. (2012). Wind Turbine Control Using PI Pitch Angle Controller. *IFAC Proceedings Volumes*, 241-246.

Karimi-Ghartemani, M. (2014). *Enhanced phase-locked loop structures for power and energy applications.* John Wiley & Sons.

Njiri, J., & Söffker, D. (2016). State-of-the-art in wind turbine control: Trends and challenges. *Renewable and Sustainable Energy Reviews*, 377-393.

Polinder, H., Ferreira, J. A., Jensen, B. B., Abrahamsen, A. B., Atallah, K., & McMahon, R. A. (2013). Trends in wind turbine generator systems. *IEEE Journal of emerging and selected topics in power electronics*, 174-185.

Sira-Ramírez, H. (2018). From flatness, GPI observers, GPI control and flat filters to observer-based ADRC. *Control Theory and Technology*, 249–260.

ISSN 2444-4987

Sira-Ramírez, H., & Agrawal, S. (2004). *Differentially flat systems.* Crc Press.

Sira-Ramírez, H., & Zurita-Bustamante, E. W. (2021). On the equivalence between ADRC and Flat Filter based controllers: A frequency domain approach. *Control Engineering Practice*.

Sira-Ramírez, H., Luviano-Juárez, A., Ramírez-Neria, M., & Zurita-Bustamante, E. W. (2017). *Active disturbance rejection control of dynamic systems: a flatness based approach.* Elsevier.

Sira-Ramirez, H., Zurita-Bustamante, E. W., & Huang, C. (2019). Equivalence among flat filters, dirty derivative-based PID controllers, ADRC, and integral reconstructor-based sliding mode control. *IEEE Transactions on Control Systems Technology*, 1696-1710.

Wu, B., Lang, Y., Zargari, N., & Kouro, S. (2011). *Power Conversion and Control of Wind Energy Systems.* John Wiley & Sons.

ISSN 2444-4987

Article **Journal of Research and Development**
June, 2021 Vol.7 No.19 22-30

Implementation of improvement actions in a company that produces frames and moldings

Implementación de acciones de mejora en una empresa que produce marcos y molduras

FORNÉS-RIVERA, René Daniel†*, CONANT-PABLOS - Marco Antonio, CANO-CARRASCO Adolfo and LÓPEZ-ROJO, Gildardo Guadalupe

Instituto Tecnológico de Sonora, Departamento de Ingeniería Industrial, Campus Ciudad Obregón, Sonora.

ID 1st Author: *René Daniel, Fornés-Rivera* / **ORC ID**: 0000-0002-7438-0056, **Researcher ID Thomson:** G-3906-2018, **arXiv Author ID**: rene_fornes, **CVU CONACYT ID**: 280435

ID 1st Co-author: *Marco Antonio, Conant-Pablos* / **ORC ID:** 0000-0002-3364-3702, **Researcher ID Thomson:** G-3911-2018, **arXiv Author ID**: Mconant, **CVU CONACYT ID**: 687331

ID 2nd Co-author: *Adolfo, Cano-Carrasco* / **ORC ID:** 0000-0002-3392-3667, **Researcher ID Thomson:** G-5035-2018, **arXiv Author ID:** adolfo. cano, **CVU CONACYT ID**: 276064

ID 3rd Co-author: *Gildardo Guadalupe, López-Rojo* / **ORC ID:** 0000-0001-7740-6613, **Researcher ID Thomson:** Gildardo Lopez, **arXiv Author ID:** Gildardo_Lopez

DOI: 10.35429/JRD.2021.19.7.22.30 Received March 26, 2021; Accepted June 24, 2021

Abstract

This research was developed in a company that manufactures frames and moldings in the production and quality area and addresses the need to implement improvement actions due to rework and low production in the patching workstation, derived from flaws such as poor patching, bump, bubble and porosity in the products. Currently there is a production record of 1.75% and rework of 19.25% in the first hours of the working day. The objective was to implement improvement actions, through the 8D's methodology, to reduce rework and increase production. The procedure implied forming a team; defining the problem; implementing containment actions; identifying and verifying the root cause; determining permanent corrective actions; identifying and implementing permanent corrective actions; preventing the recurrence of the problem and/or root cause, and acknowledging the effort of the team. It contributed with the increase in production and reduction of rework in the patching workstation, thus fulfilling the objective of this research.

Improvement actions, Implementation, 8D's

Resumen

Esta investigación se desarrolló en una empresa elaboradora de marcos y molduras en el área de producción y calidad y aborda la necesidad de implementar acciones de mejora a consecuencia de retrabajos y baja producción en la subárea de resane, derivada de defectos tales como: mal resane, golpes, burbuja y porosidad en los productos. Actualmente se tiene un registro de producción de un 1.75% y de retrabajo de un 19.25% en las primeras horas de la jornada laboral. El objetivo consistió en implementar acciones de mejora, a través de la metodología 8D´s, para reducir el retrabajo e incrementar la producción. El procedimiento fue: Formar un equipo; definir el problema; implementar acciones de contención; identificar y verificar la causa raíz; determinar acciones correctivas permanentes; identificar e implementar las acciones correctivas permanentes; prevenir la recurrencia del problema y/o causa raíz y reconocer el esfuerzo del equipo. Se contribuyó con el incremento en la producción y reducción de retrabajos en la subárea de resane, Cumpliendo así con el objetivo de esta investigación.

Acciones de mejora, Implementación, 8D´s

Citation: FORNÉS-RIVERA, René Daniel, CONANT-PABLOS - Marco Antonio, CANO-CARRASCO Adolfo and LÓPEZ-ROJO, Gildardo Guadalupe. Implementation of improvement actions in a company that produces frames and moldings. Journal of Research and Development. 2021. 7-19: 22-30

* Correspondence to Author (e-mail: rene.fornes@itson.edu.mx)
† Researcher contributing as first author.

1. Introduction

Industrialization is an economic phenomenon based on the intensive production of goods. This development, in turn implies the creation of workers increasingly prepared to tackle new tasks, as well as the adaptation of production processes to the new tasks that have appeared, preserving and increasing their productivity. (Sánchez, 2021). Productivity is the relationship between final production and productive factors used to obtain goods and services; and this should be measured as a ratio of the output divided by the input, Carro and González (2021); while for Gutiérrez and Huaman (2014), López (2018) and Vásquez (2018) productivity serves to evaluate the performance of workshops, machinery, work teams and employees.

On the other hand, for Evans and Lindsay (2020), a process is a sequence of linked activities whose objective is to achieve some result, such as producing a good or service for a client inside or outside the organization; in turn, for Louffat (2017) it is the set of sequential and integrated activities that aim to generate value for an internal or external client, through the transformation of inputs into final products or services. For Martin and Rodríguez (2019) and Torres (2019), corrective and preventive actions must be supported by the prior evaluation of the situation, so it cannot be immediate; these actions represent a proposal for improvement that arises as a consequence of having studied the cause of a non-conformity detected in the company when applying corrective and preventive actions.

For ISOTools (2016), some organizations have effective systems, each of which may have its own improvement system. Consequently, quality is achieved, which is perfection in relation to the execution of productive activities, where it is guaranteed that the product is well-made, produced on time, preserving the environment and considering worker safety (Morales and Muñoz, 2019). The organization shall consider the results of the analysis and evaluation, and the outputs of the management review, to determine if there are needs or opportunities that should be considered as part of continuous improvement (ISO 9001: 2015, 2018).

Continuous improvement is associated with a diversity of organizational developments, including the adoption of modern approaches such as Total Quality Management (TQM), Lean Manufacturing, Theory of Constraints (TOC), Six Sigma (SS), Kaizen, among others (Singh & Singh, 2015). Continuous improvement has an advantage since the standard collects valuable information and optimized processes to be able to implement continuous improvement methodologies that make synergy with the quality management system and thus be able to have better monitored processes achieving a better quality of products and services that exceed expectations and customer needs (Pava et al, 2019).

In the same way, it can be considered as a process of change, development and possibilities of improvement by applying this criterion to people and organizations, having as its origin the word Kaizen that implies continuous improvement day by day and at all times; in turn, Deming's circle seeks to raise the quality and performance level of organizations so that they are competitive, in the midst of an environment subject to constant changes; Similarly, there is a structured methodology to obtain, prioritize and evaluate Kepner-Tregoe information, also called the competitive profile matrix; there is also the Six Sigma methodology which is a set of techniques and tools for improving business processes and results; finally, the 8D's methodology (Eight Disciplines Problem Solving) which is based on the basic idea of identifying and correcting the root cause of the problem and taking actions to avoid the recurrence of the failure, devise a short-term solution and implement a long-term solution to avoids its recurrence (Bernal-Moreno, 2014).

The first to have a standard of the 8 disciplines was the United States in the period of the Second World War MIL-STD-1520, known as corrective action and disposition of non-conforming material; presented in 1974, it was used as a method to deal with non-conformities. The main objective of the method was to identify the error, examine the root cause of the problem, limit losses, prevent recurrences and reduce production costs by promoting an increase in quality (Mello de Lima, 2017 and Bosch Inc. 2013). Nowadays, it has become a standard in other organizations that are not in the automotive sector and that adopt this problem-solving methodology (SPC Group, 2020).

ISSN 2444-4987

The methodology consists of 8 actions; namely, D1: Set a team; D2: Define the problem; D3; Implement containment actions; D4: Identify and verify the root cause; D5: Determine permanent corrective actions; D6: Implement and verify permanent corrective actions; D7: Prevent the recurrence of the problem and/or its root cause; and D8: Acknowledge the efforts of the team (Mello de Lima, 2017 and Bosch Inc. 2013).

For Soto (2018) the quantification or numerical translation of the dimensions is an indicator, which must be represented clearly and precisely. According to López and Valdiviezo (2017), the indicators allow us to optimally evaluate the operation of the management system and plan activities according to the goals and objectives set by the department. The costs are implicitly stated; which for Muyulema-Allaica et al. (2020) are the unavoidable expenses to maintain a production line; and in relation to the latter; Torres (2017) maintains that the decrease in the budget limits the amount of investments programmed to keep the company at its optimal level; affecting its productivity.

The company under study is dedicated to the manufacture of mirrors, giclees, oils, lithography and sandblasting for decoration, it has a staff of 80 people between general and administrative operators. The market it serves is national and international; it includes department stores, large commercial chains, hotels, furniture stores, decoration stores and finally specific clients or exclusive projects. The production process begins with the reception of the raw material and continues with carpentry, molding, inspection, casting, patching, finishing, assembly, packaging, shipment and end customer (Alfa-*Delta, S.A. de C.V., 2019).*

In the months of January-May 2019, the company documented the processes and procedures that are carried out to have a better control over them; thus, the managers obtained real data from the areas of interest such as production and quality, deciding to attend the patching, finishing, and assembly workstations; given that it is urgent for the company to be aware of the performance, since a large number of products from the finishing and assembly workstations are sent back to the patching workstation and the reason is unknown.

This affects daily production, with the bottleneck being located in the patching workstation and the reason for this project is because this is the area that determines the production rate. In September, the processes in the different workstations were diagnosed and analyzed in order to take a sample and learn about the current situation of the company and thus be able to determine the problems to be solved along with the managers. Table 1 displays the product behavior.

Schedule	Produced amount	% Production
8-9 am	5	1.75%
9-10 am	21	7.34%
10-11 am	30	10.49%
11-12 pm	38	13.29%
12-1 pm	34	11.89%
2-3 pm	34	11.89%
3-4 pm	37	12.94%
4-5 pm	42	14.69%
5-6 pm	45	15.73%
	286	100.00%

Table 1 Production sampling of the patching area
Source: Alfa- Delta, S.A. de C.V. (2019)

As we can see, there is a low level of production at the beginning of the working day; similarly, the analysis of the flaws was carried out, see Table 2.

Flaw	Percentage of flaws
Poor patching (18/48)	37.50%
Bump (25/48)	52.08%
Bubble (3/48)	6.25%
Porosity 48 defective pieces	4.16%

Table 2 Percentage of flaws in patching
Source: Alfa- Delta, S.A. de C.V. (2019)

Once the percentage of flaws was obtained, we proceeded to obtain the percentage of rework, which consists of reducing/eliminating the errors derived from production, generating flaws such as poor patching, bumps, bubbles and porosity in aspects such as: bad sanding, bad patches in mahogany, a poor putty application, a poor patching with a filler, and an inadequate bubble extraction; see Table 3.

Total of pieces produced	286
Total of pieces with flaws	48
Percentage of rework	16.78%

Table 3 *Percentage of rework in patching*
Source: Alfa-Delta, S.A. de C.V. (2019)

ISSN 2444-4987

Because the sampling carried out was only diagnostic, the company requires a longer analysis to determine what the causes of these problems are, especially in the first hours of the working day in the patching workstation, aiming to implement improvement actions through the information obtained and analyzed, to reduce rework and increase production in the first hours of the working day in the patching workstation in the company under study.

2. Methodology to be developed

The object of study was the production process in the patching workstation in a company located in the industrial zone of Ciudad Obregón, Son. The materials were the process documentation of Morales and Muñoz (2019) and the methodology of the 8D's of Mello de Lima (2017) and Bosch Inc. (2013). The procedure was: D1) selection of the project team; D2) definition of the problem; D3) implementation of containment actions; D4) identification and verification of the root cause; D5) determination of permanent corrective actions; D6) identification and implementation of permanent corrective actions; D7) prevention of recurrence of the problem and/or root cause; and D8) acknowledgement of the team effort.

3. Results

The result obtained is presented and it contains tables, which due to their size, only a part will be presented.

D1) Formation of the project team

The work team was formed, made up of the director of operations, production, quality and two collaborators.

D2) Definition of the problem

Once established, the collaborators analyzed the information that was generated in two weeks in which four types of flaws occurred on inspection table one, see Table 4.

Flaw	Flaw percentage
Poor patching	41.40%
Bump	37.29%
Bubble	18.60%
Porosity	2.72%

Table 4 Percentage of flaws in the patching workstation

With the results obtained and with the production of the two weeks analyzed, the rework percentage was obtained, see Table 5.

Total of pieces produced	639
Total of pieces with flaws	123
Percentage of rework	19.25%

Table 5 Percentage of rework for patching

Maintaining a low production index, see Table 1, in the first hours of the working day of 1.75%.

D3) Implementation of containment actions

Once having the necessary information, two containment actions were implemented, due to the variability of production per operator, this caused by the organization in the product flow. This is where the first inputs first outputs were implemented, as can be seen in Figure 1.

Figure 1 First inputs first outputs
Source: Alfa-Delta, S.A. de C.V. (2019)

Continuing with the second containment action, the operator was changed due to his advanced age and lack of motivation in the activity carried out, resulting in the failure to identify defective parts in two consecutive weeks, being unacceptable because the activities performed by the operators involve manual work.

D4) Identification and verification of the root cause

The task of collecting information was carried out in October where the variation between what was produced in the patching workstation with a total of 1496 frames and what was produced in the assembly workstation with a total of 1321 frames is verified, which generates a gap of less than 175 frames, unknowing its location. The flaws can be seen in Table 6.

ISSN 2444-4987

Flaw	Percentage of flaws
Poor patching	30.80%
Bump	39.16%
Bubble	24.71%
Porosity	5.32%

Table 6 Flaws from October for patching

Once having identified the problems, we undertook the task of investigating what the root cause was, for this the 5W + H technique was developed in which the possible causes of the different problems were discovered starting with the bump, finding that the cause was the lack of training for the personnel to handle the product, and the lack of protections in the transport equipment, as well as a poor patching, where there was a poor training for the operators; the production problem continued, where low productivity was found at the beginning of the day, as well as a lack of supervision; as well as the implementation of a stock for the beginning of the next day. Finally, the difference between what patching produces and what assembly does was analyzed, finding the non-existent training in the handling of reworked product and that there is no special transport equipment for reworked product being the cause of ignorance of all 175 frames.

D5) Determination of permanent corrective actions

With the root causes identified, the team met with the following corrective actions:

1) Adaptation of protections to the transport equipment to reduce or eliminate the shock caused by moving the products.
2) Training of operators, to reduce the large number of rework due to damages and defects due to mishandling the product and incorrect patching.
3) Implementation of a transport equipment for rework, to reduce the variation of what is produced in the patching and assembly workstations, due to the loss of produced parts.
4) Implementation of stock at the beginning of the day: to ensure that operators have product when they arrive to their work station.

D6) Implementation and verification of permanent corrective actions

As an improvement action for the transport equipment, protective tape was applied and fom adapted to the lateral crossbar, see Figure 2.

Figure 2 Protection of transport equipment
Source: Alfa-Delta, S.A. de C.V. (2019)

Moving on to the next implemented action, which was the training of operators when they did not perform their work correctly, the operations and quality director met and trained the operators of the patching and finishing workstations; reducing the bumps and the poor patching. For the results of this, the percentage of defects within the total defects was considered, before and after the implementation of the corrective actions, see Table 7.

Flaw	Percentage of flaws
Poor patching	15.84%
Bump	10.89%
Bubble	38.61%
Porosity	34.65%

Table 7 Flaws in the patching workstation

As seen in table 7, once the corrective actions were implemented, the flaws per bump decreased from 52.08% to only 10.89% and the flaws due to poor patching went from 37.5% to 15.84%, with which the defects due to bubble and porosity became the most significant because they were testing new chemical components which were not tackled by delimitation in the present project, in addition to the fact that these, as known, are produced mainly due to the chemical reactions of the raw material used (polyurethane) by its very nature and the effect that the environment has over it. Regarding rework, there was 19.25% in the diagnosis made, with improvements in this area, see Table 8.

ISSN 2444-4987

Indicator/Month	Sep.	Oct.	Nov.
Total of pieces produced	1292	1496	1128
Total of pieces with flaws	234	263	101
Percentage of rework	18.11%	17.58%	8.95%

Table 8 Evolution of the percentage of rework

The third action was to implement a transport equipment for rework, to eliminate variation between what comes out of the patching workstation and what comes out of the assembly workstation, see Figure 3. With the production analysis, the total and the difference of frames produced in the month of November was identified, see Table 9.

	Patchig	Assembly	Difference	% Dif. * Absolute
Before	1496	1321	-175	13.25%
Now	1128	1177	+49	4.34%

Table 9 Difference between production patching-assembly
* Difference/production of the workstation with the lowest production

As seen in table 8, the implementation of the improvement action made it possible to reduce the difference in production between the areas from 13.25% to 4.34%; in addition to the fact that due to the production flow, we are able to notice that unlike before, the assembly workstation now shows an overproduction in relation to patching, which may be due to the fact that it is in the process of recovering the missing parts, which were in production, but up to this point we had not had knowledge of them.

Finally, due to the low productivity at the beginning of the day, the stock was implemented (Being a simple way to calculate it; divide the desired daily production by the working day (9 hrs) establishing the stock as the difference between the desired production average per hour, minus the average production during the first hour of the work day, example: Considering the production of the month of October of 1436 frames.

– Production first hour = 1436 (0.0175) = 25 frames
– Desired production/hr. = 1436/9 = 160 frames
– Stock = 160-25= 135 frames) of material to improve operator performance. Figure 3 shows the implemented improvement.

Figure 3 Stock for the beginning of the day
Source: Alfa-Delta, S.A. de C.V. (2019)

After the implementation of the stock for the beginning of the day, an increase in production is appreciated, see Graph 1.

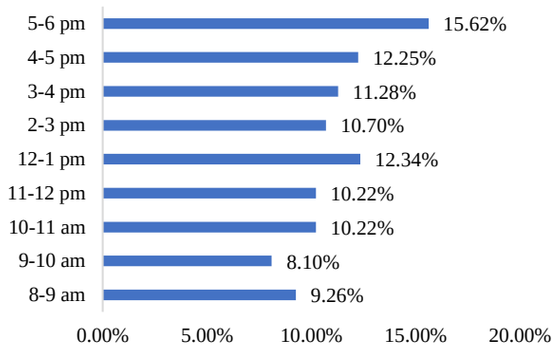

Graph 1 Production percentage of patching in November
Source: Alfa-Delta, S.A. de C.V. (2019)

Another way to see the improvement or increase in production with the implementation of the stock is the increase in daily production from 1436 to 1596 frames/day.

D7) Prevention of the recurrence of the problem and/or root cause

To avoid recurrences of the problems that were tackled by the improvements, a series of actions is shown:

a) Maintenance plan for the transport equipment. To prevent the recurrence of damage and alterations in the final product during its journey through the different areas of the production line, it is recommended to change the protective tape every three months or when it appears damaged due to wear, since this is the life-span estimated for it; on the other hand, the change of the protective fom will be carried out annually.

ISSN 2444-4987

b) Stock of raw materials to start daily work. To ensure the supply of raw material, it is observed that the initial raw material stock must be calculated (as was done previously) and the raw material count must be carried out in the last hour of the working day in this case from 5:00 pm to 6:00 pm, by a supervisor and be signed by the director of operations.

c) Staff training. We prepared a table of competencies that shows the capacities that an operator must have in order to carry out their day-to-day work, which include capacities for: a) sanding; b) putty application; c) application of mahogany patch; d) putty filler; and d) bubble extraction, with a weighting; being number one, not competent, number two, moderately competent and number three competent; as they are related to the patching workstation, the finishing workstation also designed a production format that assesses the capacities in the process of: a) grinding; b) scratching; c) classics; d) broaching; e) formulation of inks; and f) knowing how to carry out a final inspection of the product. Similarly, to the assembly area personnel: a) glass cutting; b) oil painting; c) styrene mount; and d) wallpaper.

d) Control over the reworked product. It was designed including the necessary specifications to facilitate the filling of the operator, as well as the understanding of the content for its readers, such as its area of origin (finishing or assembly) as well as the name of the operator who is working on it (this way we can also monitor performance) includes the name of the type of flaw that the product suffered and, finally, after the rework has been carried out, the name of the person who released it.

D8) Acknowledgement of the team effort

In this section, a comparative analysis was carried out of the changes that the process underwent during the months of work, thus showing the achievement obtained through the improvements proposed and implemented in the patching area:

A. Production increased at the beginning of the day from 1.75% to 9.76%
B. Parts from rework decreased from 19.25% to 8.95%
C. The most critical types of flaws addressed were:
   a. Bump, down from 52.08% to 10.89%
   b. Poor patching, went from 37.50% to 15.84%

Giving importance to the achievements obtained and encouraging those involved in the way that the company considers best will be very important for a greater involvement of the staff in the continuous improvement of processes and products.

4. Conclusion

The purpose of this project was to implement improvement actions, through the collection and analysis of information in the areas of production and quality focused on reducing rework and increasing production in the first hours of the working day. Therefore, once the project is completed and based on each of the results obtained, it is possible to mention its achievement, complying with the proposed objective. Finally, the methodology of the 8 D'S, turned out to be very practical since it allows the improvement of the product establishing a standardized practice to continue seeking to focus on the origin of each problem by determining the root cause to implement effective improvement actions. Consequently, each of the products obtained from the implemented method seeks a positive impact on the rework and production indicator in the company's patching workstation, thereby also generating a better quality in the final product.

5. Recommendations

According to the above, it is recommended to form a team which is in charge of carrying out future improvement actions, as well as carrying out new analysis to identify the causes of defects and thus achieve a continuous improvement process. In addition, it is recommended that the necessary maintenance has to be done to the transport equipment, in order to avoid their wear and tear, as well as continuing to apply training for the prevention of manual defects, either in the patching area or in the finishing, quality and production coordinators are recommended to follow up with their workers to maintain what has been achieved in this project.

ISSN 2444-4987

6. References

Alfa-Delta S.A. de C.V. (2019). *Informe general de la empresa.*

Bernal-Moreno, J.E. (2014). *Importancia de la administración y solución de problemas en el desarrollo de productos*. [Tesina. Universidad Autónoma del Estado de México]. http://ri.uaemex.mx/bitstream/handle/20.500.11799/32531/419689.pdf?sequence=2&isAllowed=y

Bosch, Inc. (2013). *Quality Management in the Bosch Group. PROBLEM SOLVING*. https://assets.bosch.com/media/global/bosch_group/purchasing_and_logistics/information_for_business_partners/downloads/quality_docs/general_regulations/bosch_publications/booklet-no16-problem-solving_EN.pdf

Carro, R. y González, D. (2021). Productividad y competitividad. Universidad Nacional del Mar de Plata http://nulan.mdp.edu.ar/1607/1/02_productividad_competitividad.pdf

Evans, J. y Lindsay, W. (2020). *Administración y control de la calidad 10a Ed.* CENGAGE. https://itson.vitalsource.com/#/books/9786075269276/cfi/4!/4/4@0:0.00Gutiérrez, H. y Huaman, A. (2014). *Influencia de la motivación laboral en la productividad en la financiera uno Oechsle - Huancayo.* (Tesis de pregrado). Universidad Nacional Del Centro Del Perú, Huancayo, Perú. http://repositorio.uncp.edu.pe/bitstream/andle/UNCP/2474/Gutierrez%20HuamanHuaman%20Araujo.pdf?sequence=1&isAllowed=y

ISO 9001:2015. (2018). *Sistema de Gestión de Calidad, fundamentos principales.* Nueva ISO 9001:2015. https://www. nueva-iso ¿9001-2015.com/2018/04/sistema-de-gestión-de-calidad-principios/

ISOTools. (2016). *OSHAS 180001: 7 pasos para realizar las acciones correctivas es un SG-SST.* https://www.isotools.cl/ohsas-180017-pasos-para-realizar-las-acciones-correctivas-en-un-sg-sst/

López, R. y Valdiviezo, C. (2017). *Optimización del sistema de gestión de mantenimiento de la maquinaria pesada del Gobierno autónomo descentralizado de la provincia del Cañar, a través de la gestión por procesos.* (Proyecto técnico de pregrado). Universidad Politécnica Salesiana Sede Cuenca, Ecuador. https://dspace.ups.edu.ec/bitstream/123456789/14308/1/UPS-CT007027.pdf

López, Z. O. *(2018). Cultura organizacional y productividad. Estudio de caso en una microempresa productora de botanas (Tesis de pregrado). Facultad de Contaduría y Administración, Metepec, México. http://ri.uaemex.mx/handle/20.500.11799/95193*

Louffat, E. (2017). *Diseño organizacional basado en procesos.* CENGAGE Learning Editores. https://itson.vitalsource.com/#/books/9786075263045/cfi/4!/4/2@100:0.00

Martin, M. y Rodriguez, J. (2019). *CAPA Acciones correctivas y preventivas en las industrias alimentarias. Díaz de Santos*. https://www.editdiazdesantos.com/wwwdat/pdf/9788490522158.pdf

Mello de Lima, T. (27 de octubre de 2017). *nucleo do conhecimento.* https://www.nucleodoconhecimento.com.br/ingenieria-de-produccion/metodologia-8d-2

Morales, K. y Muñoz, F. (2019). *Actualización de la documentación de procesos con base en la ISO 9001:2015, en una empresa elaboradora de marcos y molduras*. [Tesis no publicada] Instituto Tecnológico de Sonora. Ciudad Obregón, Sonora.

Muyulema-Allaica, C. A., Muyulema-Allaica, J. C., Pucha-Medina, P. M., y Ocaña-Parra, S. V. (2020, 01, 04). *Los costos de producción y su incidencia en la rentabilidad de una empresa avícola integrada del Ecuador: caso de estudio. Visionario Digital.* http://www.cienciadigital.org/revistacienciadigital2/index.php/VisionarioDigital/article/view/1089/2615

Pava, C. Ramírez, J. y Marín, W. (2019). *Metodologías de mejora continua integrables al sistema de gestión de calidad bajo la norma ISO 9001. Herramientas y metodologías de mejora continua aplicada al sistema de gestión de calidad bajo la norma ISO 9001*. https://repository.usc.edu.co/bitstream/h ¿ndle/20.500.12421/1311/METODOLOG%C3 %8DAS%20DE%20MEJORA.pdf? sequence=1&isAllowed=y

Sánchez, J. (2021). *Industrialización.* https://economipedia.com/definiciones/industria lizacion.html

Singh, J., & Singh, H. (2015). *Continuous improvement pholosophy – literature review and directions.* An International Journal. https://doi.org/10.1108/BIJ-06-2012-0038Soto, S. E. (2018). *Variables, dimensiones e* indicadores en una tesis. https://tesisciencia.com/2018/08/20/tesis-variables-dimensiones-indicadores/

SPC Group. (2020). 8 *Disciplinas para la solución de problemas*. https://spcgroup.com.mx/8_disciplinas_20_12_ 19/

Torres, I. (2019). Corrective actions. https://iveconsultores.com/acciones-correctivas/

Torres, R. (2017). *Proposal for the implementation of a preventive maintenance program to reduce maintenance costs, applied in the pulp plant company Trupal S.A.* (Tesis de pregrado). Universidad privada del Norte, Trujillo, Perú. de https://repositorio.upn.edu.pe/bitstream/handle/ 11537/13603/Torres%20Rojas%20Jaime%20Pa ul.pdf?sequence=1&isAllowed=y

Vásquez, P. (2018). *Estudio realizado con agentes de la PMT de la municipalidad de San Pedro Sacatepéquez, San Marcos* (Tesis de pregrado). Universidad Rafael Landívar, Quetzaltenango, Guatemala. http://recursosbiblio.url.edu.gt/tesiseortiz/2018/ 05/43/Vasquez-Mayra.pdf

Article **Journal of Research and Development**
June, 2021 Vol.7 No.19 31-36

Design and simulation of Dynamic Voltage Restorer (DVR) supported by solar panels

Diseño y simulación de un Restaurador Dinámico de Voltaje (DVR) soportado por paneles solares

ANTONIO-LARA, Omar†, GARCÍA-VITE, Pedro Martín*, CASTILLO-GUTIÉRREZ, Rafael and CISNEROS-VILLEGAS, Hermenegildo

TECNM / Instituto Tecnológico de Ciudad Madero, División de estudios de posgrado e investigación

ID 1st Author: *Omar, Antonio-Lara* / **ORC ID**: 0000-0002-5146-4820, **CVU CONACYT ID:** 1036314

ID 1st Co-author: *Pedro Martín, García-Vite* / **ORC ID**: 0000-0001-6019-7958, **CVU CONACYT ID:** 227310

ID 2nd Co-author: *Rafael, Castillo-Gutiérrez* / **ORC ID**: 0000-0001-8599-892X, **CVU CONACYT ID:** 63299

ID 3rd Co-author: *Hermenegildo, Cisneros-Villegas* / **ORC ID**: 0000-0001-7601-0449, **CVU CONACYT ID:** 63302

DOI: 10.35429/JRD.2021.19.7.31.36 Received March 17, 2021; Accepted June 30, 2021

Abstract

This work presents the design and simulation of a Dynamic Voltage Restorer (DVR) to mitigate power quality problems such as voltage sags and swells at sensitive loads to these types of disturbances, but with a compensation topology using one the most popular of the renewable energies, currently employed, which is photovoltaic solar energy. The DVR must operate with a control loop, monitoring the voltage at the load side and generating the voltage for compensation during the disturbances. The energy is obtained, from an array of solar panels for the injection of active power. The control algorithm discussed in this article is based on the Clark and Park transformations to generate the required signals for voltage compensation, these mathematical techniques allow fixing the variables and hence simplicity for the controller design. The results of the simulation in MATLAB/Simulink are used to show the performance of the proposed topology with symmetrical voltage sags in the distribution system.

Power quality, Solar energy, Voltage sag

Resumen

En este trabajo se presenta el diseño y simulación de un Restaurador Dinámico de Voltaje (DVR) para mitigar problemas de la calidad de la energía como huecos y elevaciones de tensión en cargas sensibles a este tipo de perturbaciones, pero con una topología de compensación utilizando una de las energías renovables con mayor auge actualmente, que es la energía solar fotovoltaica. El DVR debe operar con un lazo de control, monitoreando el voltaje en la carga y generando el voltaje de compensación durante el disturbio. La energía para la compensación, es obtenida de un arreglo de paneles solares para la inyección de potencia activa. El algoritmo de control discutido en este artículo se basa en las transformaciones de Clark y Park para generar las señales requeridas para la compensación de voltaje, estas herramientas matemáticas permiten fijar las variables y con ello simplicidad para el diseño del controlador. Los resultados de la simulación en MATLAB/Simulink son usados para mostrar el desempeño de la topología propuesta ante huecos de tensión simétricos en el sistema de distribución.

Calidad de la energía, Energía solar, Hueco de tensión

Citation: ANTONIO-LARA, Omar, GARCÍA-VITE, Pedro Martín, CASTILLO-GUTIÉRREZ, Rafael and CISNEROS-VILLEGAS, Hermenegildo. Design and simulation of Dynamic Voltage Restorer (DVR) supported by solar panels. Journal of Research and Development. 2021. 7-19: 31-36

* Correspondence to Author (e-mail: pedro.gv@cdmadero.tecnm.mx)
† Researcher contributing as first author.

I. Introduction

In recent years, industrial companies, as well as residential and commercial users have focused their attention on the problem of power supply quality and demand better conditions in the quality of the voltage wave, because a poor quality of supply brings considerable economic losses. Currently, the electrical distribution system has loads that are more sensitive to disturbances such as: voltage interruptions, voltage rises and dips, as a consequence of the connection and disconnection of large motors, connection of photovoltaic systems to the grid, capacitor banks, short-duration interruptions, among others.

Under these circumstances, FACTS devices used in transmission systems to improve power quality have been taken as a basis and new power conditioning devices for the distribution system (D-FACTS) have been designed to regulate and control the power flow. Such is the case of the Dynamic Voltage Restorer (DVR) which is a D-FACTS technology that is connected in series with the distribution line, being able to inject a compensation voltage with the purpose of improving the voltage quality in a sensitive load in case of system disturbances.

On the other hand, renewable energy sources are increasingly incorporated in applications where fossil fuels and their derivatives were used, since they do not produce environmental pollution and, in addition, some such as solar photovoltaic has an almost inexhaustible source to produce electricity. This paper presents an application of this renewable source, using solar panels to supply energy to the DVR and give greater depth of compensation by injecting active power.

This paper is divided into the following concepts: Section II presents in a general way the structure of the DVR supported by solar panels, and its operation. Section III discusses the control strategy proposed in this paper. Finally, Section IV presents the simulation results in MATLAB/SIMULINK to validate the proposed DVR topology to mitigate voltage dips.

II. General description of the system

The DVR is a power conditioner that is connected in series with the load through a three-phase injection transformer, connected in star primary and open secondary.

Its purpose is to mitigate dips and voltage rises that affect the sensitive load. Figure 1 shows that a test load is considered large enough to cause a voltage drop at the common coupling point (CCP), this load is controlled by switch *SW1* to simulate a disturbance in the system. A solar panel array is also connected to supply voltage at the inverter DC link voltage, but upstream of the inverter a Boost type DC-DC power converter is connected to boost the voltage generated by the panel to levels acceptable to the inverter. In addition, a passive filter is required at the inverter output to remove unwanted components in the output voltage produced by the high switching speed of the semiconductor devices that make up the inverter.

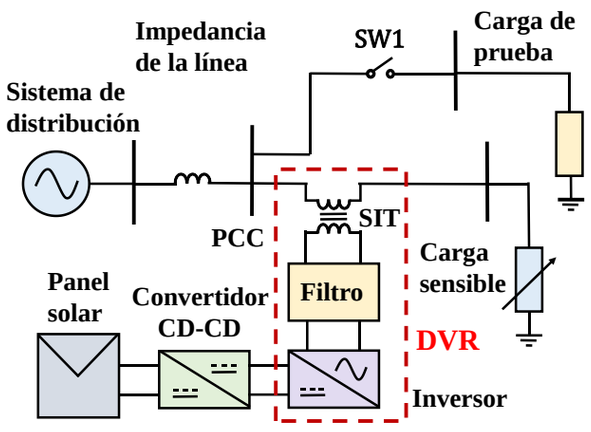

Figure 1 Block diagram of the DVR structure
Source: Own Elaboration

The operating principle of the DVR is to inject the compensation voltage V_{iny} by means of a three-phase injection transformer (SIT), together with the supply voltage V_s in order to mitigate voltage dips on the load side V_{carga}(Figure 2).

At all times the control algorithm compares the voltage at the load with a reference voltage and the difference between these two signals is considered the compensation voltage signal V_{com}, which is directly proportional to the voltage to be injected by the inverter V_{iny}. V_{com} is a digital input signal for pulse width modulation (PWM) to control the voltage source converter (inverter). The inverter converts the DC power from the solar panels to AC voltage for injection when a load disturbance occurs. And the DC-DC converter controls and regulates the required DC voltage.

ISSN 2444-4987

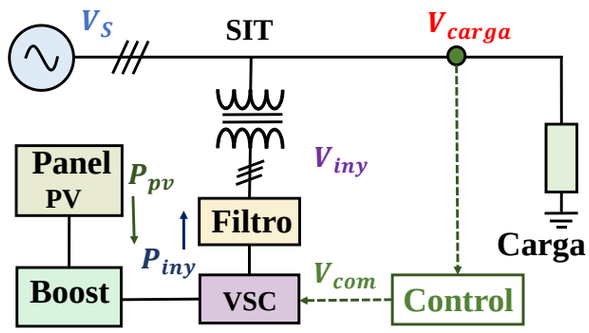

Figure 2 Simplified DVR schematic
Source: Own Elaboration

III. DVR Control

One of the requirements of the DVR is that it must operate in real time, that is, the compensation process must be executed immediately after the fault occurs without time delay, the speed of response is an essential feature in this device. The variables required for the control are the voltage measured directly at the load, and as output will be obtained the SPWM pulses going to the inverter. In this article the control algorithm implemented is based on the DQ transform (dq0- direct-quadrature-zero), this is a very useful mathematical transform used to simplify the analysis of three-phase circuits. The *dq0* transform is called Park transform and this is complementary with the Clark or αβ transform.

Clark and Park transforms.

The Clark transform or αβ transform offers the advantage of reducing the order of the space in which three-phase signals are represented from 3 to 2. In matrix form one has:

$$\begin{bmatrix} V_\alpha \\ V_\beta \end{bmatrix} = \sqrt{\frac{2}{3}} \begin{bmatrix} 1 & -0.5 & -0.5 \\ 0 & -0.866 & 0.866 \end{bmatrix} \begin{bmatrix} V_a \\ V_b \\ V_c \end{bmatrix} \quad (1)$$

The contants in (1) are obtained from the trigonometric functions of the angles of the different phases, i.e:

$$\sin(60) = \frac{\sqrt{3}}{2} \approx 0.8660$$

$$\cos(60) = \frac{1}{2} = 0.5$$

It can also be represented in the form of blocks (1) as shown in Figure 3.

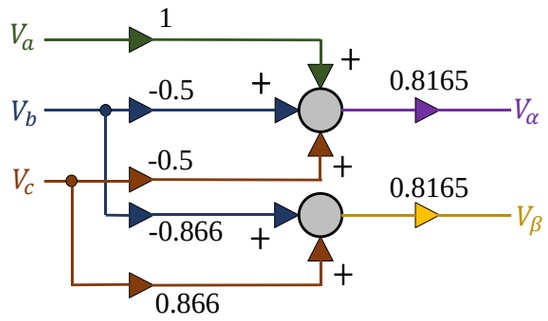

Figure 3 Transformation block abc-αβ
Source: Own Elaboration

When applying a feedback control it is highly desirable to do so with signals that do not vary with time, however, the components in αβ vary sinusoidally. For this, the Park transform is used, which has as input the vector integrated in the reference frame αβ, and as output a vector in the reference frame *dq*, whose components are constant in time. The Park transform can be expressed as:

$$\begin{bmatrix} V_d \\ V_q \end{bmatrix} = \begin{bmatrix} \cos\theta & \sin\theta \\ -\sin\theta & \cos\theta \end{bmatrix} \begin{bmatrix} V_\alpha \\ V_\beta \end{bmatrix} \quad (2)$$

Generally in practical applications (2) is not used but the inverse Park's transform, in order to inject a signal in phase or quadrature with the signal taken as reference. The finite inverse transform dq is expressed as:

$$\begin{bmatrix} V_\alpha \\ V_\beta \end{bmatrix} = \begin{bmatrix} \cos\theta & -\sin\theta \\ \sin\theta & \cos\theta \end{bmatrix} \begin{bmatrix} V_d \\ V_q \end{bmatrix} \quad (3)$$

The block representation of (3) is shown in Figure 4.

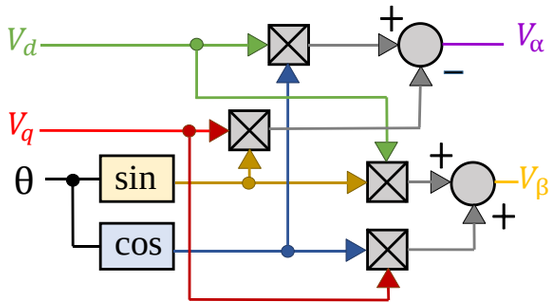

Figure 4 Inverse transformation block dq
Source: Own Elaboration

Schematic of the proposed controller

For three-phase systems it is also required to find the value of the angle θ of the reference vector to be evaluated in the inverse transform. For this purpose, a phase-locked loop "PLL" is used, this is responsible for measuring the angle of the reference vector against the α-axis, and thereby evaluating the inverse Park's transform. Figure 5 shows the control scheme used.

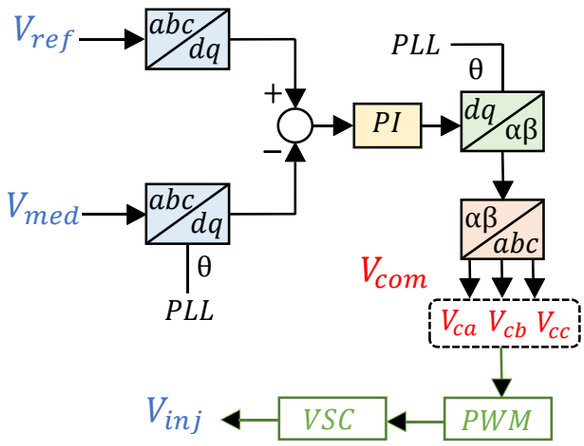

Figure 5 Proposed control scheme
Source: Own Elaboration

The way the control circuit operates as shown in Figure 5 is to first measure the three-phase voltage at the load V_{med}. Then these values are transformed to a reference frame dq and these in turn compared with a reference value V_{ref} which is the desired value of the voltage at the load. The difference or error enters a PI regulator, this controller regulates the compensation voltage V_{com}which is transformed back to an *abc* system, and the resulting voltage signals are directly sent to the switching system of the PWM inverter switches.

The SPWM signals are used for switching the semiconductor devices that make up the voltage inverter, and this generates the voltage to be injected in series with the distribution line V_{iny}through the injection transformers.

IV Simulation Results

In order to understand the performance of the DVR under voltage dips, a low voltage distribution network is simulated in MATLAB/SIMULINK (Figure 6).

This DVR uses a three-phase injection transformer consisting of three single-phase transformers in primary-star and secondary series connection, whose transformation ratio is 1:1.

In addition, a three-phase PWM voltage inverter to which an LCR filter is connected to its output to eliminate the high frequency components in the inverter output voltage. Table 1 specifies the overall system parameters.

It is worth mentioning that this article considers the photovoltaic modules operating in ideal mode, i.e., they operate with a constant temperature and irradiance of 25°C and 1000 W/m^2, so they will always deliver the maximum power according to the specifications.

Parameter	Symbol	Value
System voltage	V_S	220 V
Frequency	f	60 Hz
Active load power	P_{carga}	1 kW
Power factor	fdp	0.8 (-)
Load resistance	R_{carga}	30.97 Ω
Load inductance	L_{carga}	61.6 mH
Filter resistance	R_{filtro}	1000 Ω
Filter inductance	L_{filtro}	3.3 mH
Filter capacitance	C_{filtro}	4.7 µF
PV panel power	P_{pv}	80 W
Number of panels in series	N_s	3
Number of panels in parallel	N_p	1
Comprehensive income	K_i	5721
Proportional gain	K_p	-0.004

Table 1 DVR parameters
Source: Own Elaboration

Figure 7a shows a three-phase symmetrical voltage dip of 0.7 p. u ranging from 50 to 116 milliseconds at the system voltage source.

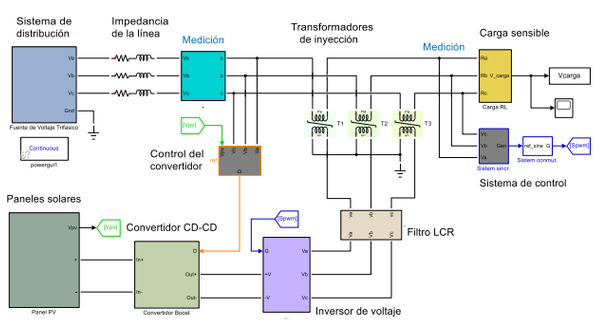

Figure 6 DVR implemented in MATLAB/Simulink

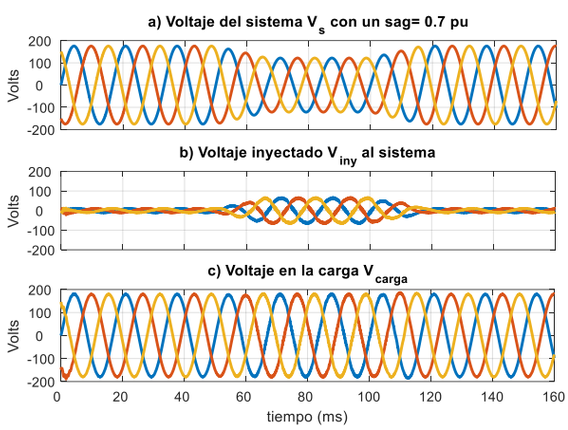

Figure 7 Voltages at a voltage dip
Source: MATLAB/Simulink

The compensation voltage provided by the injection transformers, and generated by the control system is shown in Figure 7b, and the voltage at the compensated load is observed in Figure 7c.

In order to support deep voltage dips, the solar panel system is sized with a series-parallel configuration; 3 panels in series and 1 in parallel, all 80Wpico modules. Figure 8 shows the power delivered by the array of panels and the power delivered by the Boost converter, note that these have close values because the DC-DC converter operates in an ideal way.

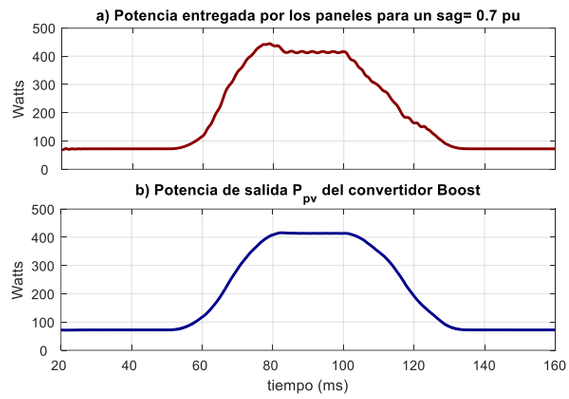

Figure 8 Instantaneous power delivered by the panels
Source: MATLAB/Simulink

The instantaneous active power at the occurrence of the voltage dip, and the one afterwards with the compensation at the load is visualized in Figure 9.

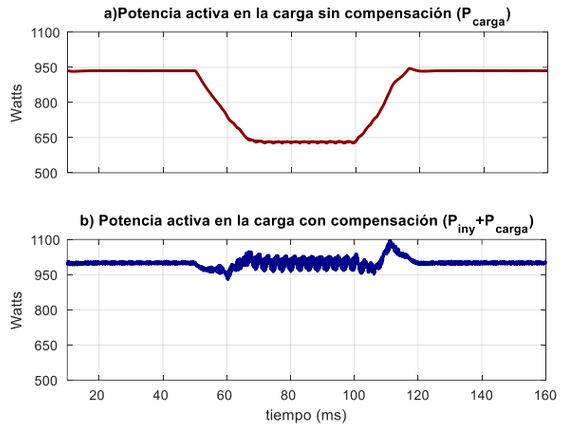

Figure 9 Active power in the load.
Source: MATLAB/Simulink

The voltage at the terminals of the panel array (V_{pv}) can be seen in Figure 10 and it is observed that the voltage is practically constant, while the voltage at the output of the boost converter or Boost (V_{boost}) increases when the symmetrical voltage gap occurs in the system, this DC-DC converter raises the voltage from the panels to levels required for compensation through the control system of the converter, varying the duty cycle (D) depending on the voltage required to inject the inverter to the system. The duty cycle variation is shown in Figure 11. Before and after the voltage dip occurs, the boost converter maintains a constant duty cycle in order to operate in continuous conduction mode.

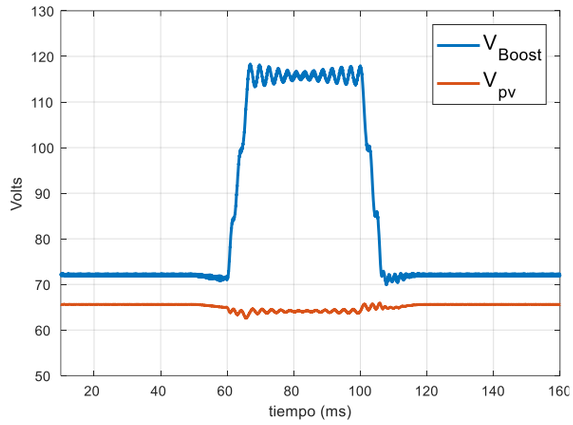

Figure 10 Panel voltage and Boost converter output voltage
Source: MATLAB/Simulink

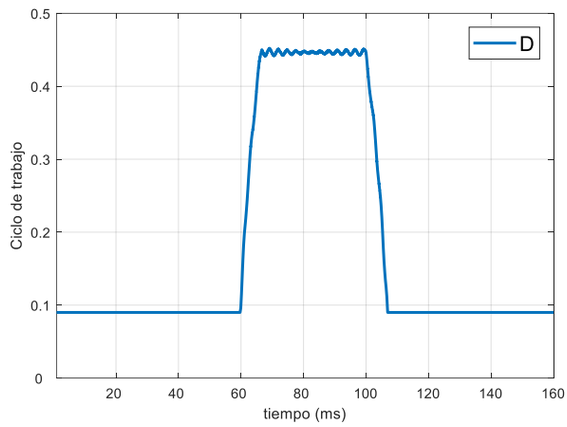

Figure 11 Duty cycle applied to the Boost Converter *Source: MATLAB/Simulink*

Acknowledgments

The authors would like to thank the Tecnológico Nacional de México campus Ciudad Madero and CONACYT with grant number (758746) for the support for the development of this project.

Conclusions

In this paper, a topology with solar panels was presented to provide support to the DVR against symmetrical voltage dips and to achieve greater compensation depth by injecting active power. Simulation results performed in MATLAB/SIMULINK demonstrate the effectiveness of the proposed structure against this type of disturbances. It is worth mentioning that for future work an energy storage system could be added to improve the system, such as batteries and/or a capacitor bank, the latter to have the possibility of injecting reactive power.

References

Nguyen Van Minh, Bach Quoc Khanh y Pham Viet Phuong, "Comparative simulation results of DVR and D-STATCOM to improve voltage quality in distributed power system," 2017 International Conference on System Science and Engineering (ICSSE), 2017, pp. 196-199.

D. Szabó, R. Bodnár, M. Regul'a y J. Altus, "Designing and modelling of a DVR in Matlab," Proceedings of the 2014 15th International Scientific Conference on Electric Power Engineering (EPE), 2014, pp. 229-233.

P. M. Garcia-Vite, F. Mancilla-David y J. M. Ramirez, "Dynamic modeling and control of an AC-link dynamic voltage restorer," 2011 IEEE International Symposium on Industrial Electronics, 2011, pp. 1615-1620.

Julio C. Rosas-Caro, Juan M. Ramírez, Pedro M. Vite García, Antonio Valderrábano y Nojja V.Vanegas Méndez. "Control de acondicionadores de potencia y dispositivos FACTS".

M. N. Tandjaoui, C. Benachaiba, O. Abdelkhalek, M. L. Doumbia e Y. Mouloudi, "Sensitive loads voltage improvement using Dynamic Voltage Restorer," Proceedings of the 2011 International Conference on Electrical Engineering and Informatics, 2011, pp. 1-5.

R. A. Kantaria, S. K. Joshi y K. R. Siddhapura, "A novel technique for mitigation of voltage sag/swell by Dynamic Voltage Restorer (DVR)," 2010 IEEE International Conference on Electro/Information Technology, 2010, pp. 1-4.

ISSN 2444-4987

[Title in Times New Roman and Bold No. 14 in English and Spanish]

Surname (IN UPPERCASE), Name 1st Author†*, Surname (IN UPPERCASE), Name 1st Coauthor, Surname (IN UPPERCASE), Name 2nd Coauthor and Surname (IN UPPERCASE), Name 3rd Coauthor

Institutional Affiliation of Author including Dependency (No.10 Times New Roman and Italic)

International Identification of Science - Technology and Innovation

ID 1st Author: (ORC ID - Researcher ID Thomson, arXiv Author ID - PubMed Author ID - Open ID) and CVU 1st author: (Scholar-PNPC or SNI-CONACYT) (No.10 Times New Roman)

ID 1st Coauthor: (ORC ID - Researcher ID Thomson, arXiv Author ID - PubMed Author ID - Open ID) and CVU 1st coauthor: (Scholar or SNI) (No.10 Times New Roman)

ID 2nd Coauthor: (ORC ID - Researcher ID Thomson, arXiv Author ID - PubMed Author ID - Open ID) and CVU 2nd coauthor: (Scholar or SNI) (No.10 Times New Roman)

ID 3rd Coauthor: (ORC ID - Researcher ID Thomson, arXiv Author ID - PubMed Author ID - Open ID) and CVU 3rd coauthor: (Scholar or SNI) (No.10 Times New Roman)

(Report Submission Date: Month, Day, and Year); Accepted (Insert date of Acceptance: Use Only ECORFAN)

Abstract (In English, 150-200 words)

Objectives
Methodology
Contribution

Abstract (In Spanish, 150-200 words)

Objectives
Methodology
Contribution

Keywords (In English)

Indicate 3 keywords in Times New Roman and Bold No. 10

Keywords (In Spanish)

Indicate 3 keywords in Times New Roman and Bold No. 10

Citation: Surname (IN UPPERCASE), Name 1st Author, Surname (IN UPPERCASE), Name 1st Coauthor, Surname (IN UPPERCASE), Name 2nd Coauthor and Surname (IN UPPERCASE), Name 3rd Coauthor. Paper Title. Journal of Research and Development. Year 1-1: 1-11 [Times New Roman No.10]

* Correspondence to Author (example@example.org)
† Researcher contributing as first author.

Introduction

Text in Times New Roman No.12, single space.

General explanation of the subject and explain why it is important.

What is your added value with respect to other techniques?

Clearly focus each of its features

Clearly explain the problem to be solved and the central hypothesis.

Explanation of sections Article.

Development of headings and subheadings of the article with subsequent numbers

[Title No.12 in Times New Roman, single spaced and bold]

Products in development No.12 Times New Roman, single spaced.

Including graphs, figures and tables-Editable

In the article content any graphic, table and figure should be editable formats that can change size, type and number of letter, for the purposes of edition, these must be high quality, not pixelated and should be noticeable even reducing image scale.

[Indicating the title at the bottom with No.10 and Times New Roman Bold]

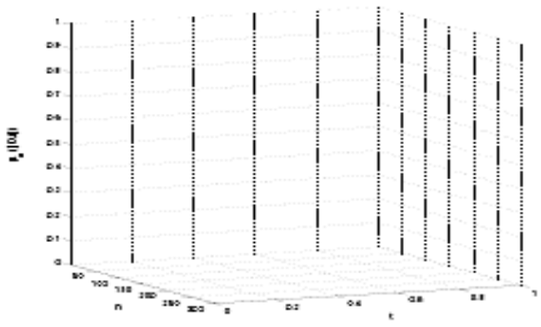

Graphic 1 Title and *Source (in italics)*

Should not be images-everything must be editable.

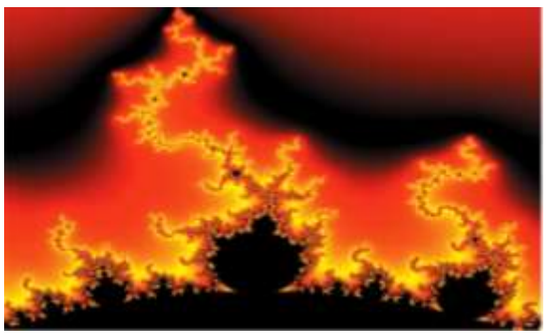

Figure 1 Title and *Source (in italics)*

Should not be images-everything must be editable.

Table 1 Title and *Source (in italics)*

Should not be images-everything must be editable.

Each article shall present separately in **3 folders**: a) Figures, b) Charts and c) Tables in .JPG format, indicating the number and sequential Bold Title.

For the use of equations, noted as follows:

$$Y_{ij} = \alpha + \sum_{h=1}^{r} \beta_h X_{hij} + u_j + e_{ij} \qquad (1)$$

Must be editable and number aligned on the right side.

Methodology

Develop give the meaning of the variables in linear writing and important is the comparison of the used criteria.

Results

The results shall be by section of the article.

Annexes

Tables and adequate sources

Thanks

Indicate if they were financed by any institution, University or company.

Conclusions

ISSN 2444-4987

Explain clearly the results and possibilities of improvement.

References

Use APA system. Should not be numbered, nor with bullets, however if necessary numbering will be because reference or mention is made somewhere in the Article.

Use Roman Alphabet, all references you have used must be in the Roman Alphabet, even if you have quoted an Article, book in any of the official languages of the United Nations (English, French, German, Chinese, Russian, Portuguese, Italian, Spanish, Arabic), you must write the reference in Roman script and not in any of the official languages.

Technical Specifications

Each article must submit your dates into a Word document (.docx):

Journal Name
Article title
Abstract
Keywords
Article sections, for example:

1. Introduction
2. Description of the method
3. Analysis from the regression demand curve
4. Results
5. Thanks
6. Conclusions
7. References

Author Name (s)
Email Correspondence to Author
References

Intellectual Property Requirements for editing:

-Authentic Signature in Color of Originality Format Author and Coauthors

-Authentic Signature in Color of the Acceptance Format of Author and Coauthors

ISSN 2444-4987

Reservation to Editorial Policy

Journal of Research and Development reserves the right to make editorial changes required to adapt the Articles to the Editorial Policy of the Journal. Once the Article is accepted in its final version, the Journal will send the author the proofs for review. ECORFAN® will only accept the correction of errata and errors or omissions arising from the editing process of the Journal, reserving in full the copyrights and content dissemination. No deletions, substitutions or additions that alter the formation of the Article will be accepted.

Code of Ethics - Good Practices and Declaration of Solution to Editorial Conflicts

Declaration of Originality and unpublished character of the Article, of Authors, on the obtaining of data and interpretation of results, Acknowledgments, Conflict of interests, Assignment of rights and Distribution

The ECORFAN-Mexico, S.C Management claims to Authors of Articles that its content must be original, unpublished and of Scientific, Technological and Innovation content to be submitted for evaluation.

The Authors signing the Article must be the same that have contributed to its conception, realization and development, as well as obtaining the data, interpreting the results, drafting and reviewing it. The Corresponding Author of the proposed Article will request the form that follows.

Article title:

– The sending of an Article to Journal of Research and Development emanates the commitment of the author not to submit it simultaneously to the consideration of other series publications for it must complement the Format of Originality for its Article, unless it is rejected by the Arbitration Committee, it may be withdrawn.

– None of the data presented in this article has been plagiarized or invented. The original data are clearly distinguished from those already published. And it is known of the test in PLAGSCAN if a level of plagiarism is detected Positive will not proceed to arbitrate.

– References are cited on which the information contained in the Article is based, as well as theories and data from other previously published Articles.

– The authors sign the Format of Authorization for their Article to be disseminated by means that ECORFAN-Mexico, S.C. In its Holding Spain considers pertinent for disclosure and diffusion of its Article its Rights of Work.

– Consent has been obtained from those who have contributed unpublished data obtained through verbal or written communication, and such communication and Authorship are adequately identified.

– The Author and Co-Authors who sign this work have participated in its planning, design and execution, as well as in the interpretation of the results. They also critically reviewed the paper, approved its final version and agreed with its publication.

– No signature responsible for the work has been omitted and the criteria of Scientific Authorization are satisfied.

– The results of this Article have been interpreted objectively. Any results contrary to the point of view of those who sign are exposed and discussed in the Article.

Copyright and Access

The publication of this Article supposes the transfer of the copyright to ECORFAN-Mexico, SC in its Holding Spain for its Journal of Research and Development, which reserves the right to distribute on the Web the published version of the Article and the making available of the Article in This format supposes for its Authors the fulfilment of what is established in the Law of Science and Technology of the United Mexican States, regarding the obligation to allow access to the results of Scientific Research.

Article Title:

Name and Surnames of the Contact Author and the Coauthors	Signature
1.	
2.	
3.	
4.	

Principles of Ethics and Declaration of Solution to Editorial Conflicts

Editor Responsibilities

The Publisher undertakes to guarantee the confidentiality of the evaluation process, it may not disclose to the Arbitrators the identity of the Authors, nor may it reveal the identity of the Arbitrators at any time.

The Editor assumes the responsibility to properly inform the Author of the stage of the editorial process in which the text is sent, as well as the resolutions of Double-Blind Review.

The Editor should evaluate manuscripts and their intellectual content without distinction of race, gender, sexual orientation, religious beliefs, ethnicity, nationality, or the political philosophy of the Authors.

The Editor and his editing team of ECORFAN® Holdings will not disclose any information about Articles submitted to anyone other than the corresponding Author.

The Editor should make fair and impartial decisions and ensure a fair Double-Blind Review.

Responsibilities of the Editorial Board

The description of the peer review processes is made known by the Editorial Board in order that the Authors know what the evaluation criteria are and will always be willing to justify any controversy in the evaluation process. In case of Plagiarism Detection to the Article the Committee notifies the Authors for Violation to the Right of Scientific, Technological and Innovation Authorization.

Responsibilities of the Arbitration Committee

The Arbitrators undertake to notify about any unethical conduct by the Authors and to indicate all the information that may be reason to reject the publication of the Articles. In addition, they must undertake to keep confidential information related to the Articles they evaluate.

Any manuscript received for your arbitration must be treated as confidential, should not be displayed or discussed with other experts, except with the permission of the Editor.

The Arbitrators must be conducted objectively, any personal criticism of the Author is inappropriate.

The Arbitrators must express their points of view with clarity and with valid arguments that contribute to the Scientific, Technological and Innovation of the Author.

The Arbitrators should not evaluate manuscripts in which they have conflicts of interest and have been notified to the Editor before submitting the Article for Double-Blind Review.

Responsibilities of the Authors

Authors must guarantee that their articles are the product of their original work and that the data has been obtained ethically.

Authors must ensure that they have not been previously published or that they are not considered in another serial publication.

Authors must strictly follow the rules for the publication of Defined Articles by the Editorial Board.

The authors have requested that the text in all its forms be an unethical editorial behavior and is unacceptable, consequently, any manuscript that incurs in plagiarism is eliminated and not considered for publication.

Authors should cite publications that have been influential in the nature of the Article submitted to arbitration.

Information services

Indexation - Bases and Repositories

LATINDEX (Scientific Journals of Latin America, Spain and Portugal)
RESEARCH GATE (Germany)
GOOGLE SCHOLAR (Citation indices-Google)
REDIB (Ibero-American Network of Innovation and Scientific Knowledge- CSIC)
MENDELEY (Bibliographic References Manager)

Publishing Services

Citation and Index Identification H
Management of Originality Format and Authorization
Testing Article with PLAGSCAN
Article Evaluation
Certificate of Double-Blind Review
Article Edition
Web layout
Indexing and Repository
ArticleTranslation
Article Publication
Certificate of Article
Service Billing

1Editorial Policy and Management

38 Matacerquillas, CP-28411. Moralzarzal –Madrid-España. Phones: +52 1 55 6159 2296, +52 1 55 1260 0355, +52 1 55 6034 9181; Email: contact@ecorfan.org www.ecorfan.org

Journal of Research and Development

2444 4987
ISSN 2444 - 4987
www.ecorfan.org